International Atomic Energy Agency

INDC(CCP)-221/L

INDC

INTERNATIONAL NUCLEAR DATA COMMITTEE

TRANSLATION OF SELECTED PAPERS PUBLISHED IN NUCLEAR CONSTANTS, VOLUME 3(52), MOSCOW 1983

Translated by the IAEA

November 1984

IAEA NUCLEAR DATA SECTION, WAGRAMERSTRASSE 5, A-1400 VIENNA

TRANSLATION OF SELECTED PAPERS PUBLISHED IN NUCLEAR CONSTANTS, VOLUME 3(52), MOSCOW 1983

Abstract

Translation of 8 papers, selected for their nuclear data interest, which were published in "Topics in Atomic Science and Technology", Series Nuclear Constants, Volume 3(52), Moscow (1983). The original report was distributed as INDC(CCP)-218/G.

Translated by the IAEA

November 1984

Reproduced by the IAEA in Austria
November 1984

84-06217

Table of Contents

Translated from Russian

UDC 539.172.4

A THEORETICAL MODEL ANALYSIS OF NUCLEAR REACTION CROSS-SECTIONS AT INTERMEDIATE ENERGIES

V.M. Bychkov, A.B. Pashchenko and V.I. Plyaskin

The phenomenological theory of nuclear reactions at intermediate energies ($E \leq 50$ MeV) is now based on various models of the reaction mechanism. The formation and subsequent decay of the compound nucleus in the general case makes a major contribution to the total interaction cross-section. The Hauser-Feshbach-Moldauer formation [1] is the most consistent method of calculating the cross-section of this process in terms of the statistical theory. Another category of reaction is the direct interaction which takes place without forming an intermediate long-lived compound nucleus system. The relative contributions of the different mechanisms may vary according to the reaction conditions and the type of interacting particles. The exiton model of pre-equilibrium decay has recently been widely used to describe that fraction of the nuclear interaction which remains after separation of the compound mechanism [2]. It seems that the exiton model can be used in the same way as the statistical approach for describing the average total contribution of direct processes [3]. Despite the well-known shortcomings of this model, it can be used to evaluate the integral contribution by direct processes over a wide energy range and for various types of interacting particles.

Thus, over the incident particle energy range examined, the integral cross-sections and the emission spectra of reaction products for a wide range of reactions can, in theory, be described by using a combination of statistical and pre-equilibrium models. Several papers have been published demonstrating how such an approach can satisfactorily describe particle emission spectra and excitation functions of reactions in the separate reaction channels [4 and 5]. In particular, the present authors have made a theoretical analysis of experimental data on neutron threshold reactions [5]. The calculations were based on the Weisskopf evaporation model and the Griffin exiton model. This analysis showed that existing experimental data could be described satisfactorily but that different systematics had to be chosen for the level density parameters in order to describe the reactions (n,p) and (n,2n). Since the result may be

distorted by imperfections in the theory applied (the Weisskopf model does not take account of the conservation of angular momentum and parity in a nuclear reaction), these findings must clearly be checked using a more accurate theory.

The main objective of this paper is to see whether a single theoretical description of nuclear reaction cross-sections and particle emission spectra can be found which is applicable to the different types of nuclear reactions.

Calculation method and parameters. The basic principle of the method used here to calculate nuclear reaction cross-sections is the division of the probability of nuclear interaction into two independent components: the formation and subsequent decay of the compound nucleus and the direct interaction. The cross-section of the nuclear reaction (a,b) using this method is written as $\sigma_{ab}(E_a, E_b) = q\sigma^{0}_{ab}(E_a, E_b) + \sigma^{\pi}_{ab}(E_a, E_b)$. Here, the first term in the equation is the probability of an interaction leading to the formation of a compound nucleus, which is calculated using the statistical theory; the second term describes the integral contribution of the direct processes, which is described by means of the exiton model. Since the compound part of the reaction is calculated using transmission coefficients obtained from a single-channel optical model, the coefficient q, which will be defined later, is needed to normalize the optical cross-section for formation of the compound nucleus taking into account the probability of the direct processes.

It is assumed that at high excitation energies of the compound nucleus, successive evaporation of the secondary particles takes place. The probability of the cascade-type particle emission is calculated using the statistical theory. It is assumed that the probability of direct processes with emission of two or more particles is small and can be disregarded. Specific calculations have been performed using the STAPRE program [6]. The program makes it possible to calculate up to six cascades of successive secondary particle emission from the compound nucleus taking into account four competitive channels, including gamma transitions. The calculation of the probability of transitions taking place for all the cascades studied is calculated with allowance for the conservation of momentum and parity laws. The population of the state with the quantum numbers (E', I', Π') of the compound nucleus i + 1 is determined by WB_{i+1}:

$$WB_{i+1}(E',I',\pi')\Delta E' = \sum_{I\pi}\int_{E'+B_i}^{E_{max}} dE\,\overline{WB}_i(E,I,\pi)\,\frac{\Gamma_i(E,I,\pi;E',I',\pi')}{\Gamma(E,I,\pi)}\,\rho_i(E',I',\pi')\Delta E'.$$

Here, $\overline{WB}_i(E,I,\Pi)$ is the population of the state (E,I,Π) in the i-th compound nucleus taking into account cascade gamma transitions; B_i is the binding energy of the particles emitted from the i-th compound nucleus; $\Gamma_i(E,I,\Pi;\ E',I',\Pi')/[\Gamma(E,I,\Pi)]$ is the probability of the transition under consideration, which is determined by the corresponding transmission coefficients; $\rho_i(E',I',\Pi')$ is the level density of the (i+1)-th compound nucleus. For discrete levels, this value is determined by: $\rho(E,\ I,\ \pi) = \sum_i \delta(E-E_i)\,\delta_{II_i}\,\delta_{\pi\pi_i}$. The probability ratios for the population of the states of the first and second compound nucleus are modified when the pre-equilibrium emission of particles is taken into account. The state of the first compound nucleus can become populated only as a result of gamma transition with a probability

$$WB_1(E,I,\pi)\Delta E = q\,\frac{\partial\sigma_{ax}^{x\phi}(E,I,\pi)}{\partial E}\,\Delta E\ ,$$

where q is a factor allowing for the reduced probability of the equilibrium phase of the compound nucleus forming as a result of pre-equilibrium emission. The population of the states of the second nucleus as a result of particle emission in the first reaction cascade is determined as follows:

$$WB_2(E,I,\pi)\Delta E = \left\{ q\,\frac{\partial\sigma_{ab}^{x\phi}(E,I,\pi)}{\partial E} + \frac{\partial\sigma_{ab}^{pre}}{\partial E}\,\frac{\left[\partial\sigma_{ab}^{x\phi}(E,I,\pi)\right]\Big/\partial E}{\sum_{I'\pi'}\left[\partial\sigma_{ab}^{x\phi}(E',I',\pi')\right]\Big/\partial E} \right\}\Delta E.$$

The probability of transition according to the compound nucleus theory is calculated as:

$$\frac{\partial\sigma^{x\phi}(E',I',\pi')}{\partial E}\Delta E' = \frac{\pi}{k_a^2}\sum_{I_c\pi_c} g^{I_c\pi_c}\,\frac{T_a^{I_c\pi_c}\,T_b^{I_c\pi_c}}{D_{I_c\pi_c}}\,\rho(E',I',\pi')\,S_{ab}^{I\pi}\,\Delta E',$$

where $S_{ab}^{I\Pi}$ is the correction for fluctuation;

$$D_{I_c\pi_c} = \sum_{b'I'\pi'}\int_0^{E+Q_{ab'}} d\varepsilon_{b'}\,T_{b'}^{I_c\pi_c}\,\rho(U_{b'},I',\pi') + \sum_{I'\pi'}\int_0^{E} d\varepsilon_f\,T_\Delta^{I_c\pi_c}\,\rho_f(U_f,I',\pi').$$

The pre-equilibrium component of the reaction is calculated from the following relationship:

$$\frac{\partial \sigma_{ab}^{pre}}{\partial \varepsilon} d\varepsilon = \sigma_a \sum_k \sum_n b_{(n)}^{(k)} \frac{\lambda_{z_i}^e(n, \varepsilon_z)}{\lambda(n)} d\varepsilon ,$$

where σ_a is the particle absorption cross-section; $b_{(n)}^{(k)}$ is the probability of population of the n-exiton state as a result of k intranuclear transitions; $\lambda_{\nu}^{e}(n, \varepsilon_{\ell})$ is the rate of transitions from the n-exiton state to a continuum; $\lambda(n)$ is the total rate of decay. The rate of intranuclear transitions is proportional to the square of the effective matrix element $/M/^2$ and the density of the exiton states. The rate of transitions from the n to the (n+2) exiton state may be written as $\lambda_+(n) = 2\pi/\hbar \left[\overline{/M/^2}\right] \times (g^3 E^2)/(p + h + 1)$.

The matrix element is determined as follows: $/M/^2 = FMA^{-3}E^{-1}$, where FM is the parameter chosen from the description of the experimental data.

The density of the exiton states is determined from the density of one-particle states g, which is related to the level density parameter in the Fermi-gas model: $g = (6/\pi^2)a$. The reduced probability of the equilibrium state of the compound nucleus forming as a result of pre-equilibrium particle emission is expressed by the factor q: $q = 1 - \sum_k \sum_n b_{(n)}^{(k)} \frac{\lambda^e(n)}{\lambda(n)}$; $\lambda^e(n) = \sum_z \int_E d\varepsilon_z \lambda^e(n, \varepsilon_z)$.

This paper examines the influence on nuclear reactions of various particles: protons, neutrons, and $^4_2$He nuclei. Their different systematics were used as calculation parameters in order to avoid adjusting the parameters and to prevent them influencing the final result. Selection of the parameters of the Fermi-gas nuclear level density model was based on the recommendations in Refs [7 and 8].

It is well known that the total contribution of the direct reaction mechanism to the cross-section is a weak function of the individual properties of the nuclei. Therefore, the pre-equilibrium emission coefficient (proportional to the interaction matrix element) was redetermined so that it did not depend on variations in the level density parameter for each specific nucleus. For this purpose, we used a normalization to the constant coefficient $\alpha = /M/^2 g^4/A$, was used which was determined from analysis of the neutron emission spectra [9] and the (n,p) reaction cross-sections [10]. The low-level systems used in the calculations were taken from Lederer's table [11], while the binding energies of the neutrons, protons and alpha-particles in the compound and residual nuclei were taken from Ref. [12].

Analysis of the calculation results. As has already been pointed out in the introduction, it is worth evaluating the difference between the results of calculations of the reaction excitation functions and the particle emission spectra based on the Weisskopf evaporation model and those based on the Hauser-Feshbach ratios. The neutron emission spectra from the reaction $^{56}Fe(n,2n)$ for energy values of 14.5 and 20.6 MeV incident neutrons obtained from these two methods are shown in Fig. 1. A single set of level density and optical potential parameters was used in the calculations and this permitted fairly accurate comparison of results. The greatest differences in the shape of the spectrum of the secondary neutron from the (n,2n) reaction are seen at the initial energy of 3.3 MeV above the (n,2n) reaction threshold. Calculation using the Hauser-Feshbach theory gives lower values in the region of low energies for the emitted neutron on account of prohibition with respect to angular momentum transferred by the neutron. For spectra at an initial energy of 20.5 MeV equivalent to 9.3 MeV above the (n,2n) reaction threshold, the results obtained by using the different methods agree reasonably well. This corresponds to the case where a large number of the ^{55}Fe residual nucleus levels are excited and the statistical approach for describing the level density is justified.

Partial cross-sections of the (n,2n) reaction with excitation of separate residual nucleus levels can provide valuable information for the study of the reaction mechanism. There are few experimental results of this type; in the case of the $^{56}Fe(n,2n)^{55}Fe$ reaction the only data on the cross-section of the population of the ground state of the nucleus ^{55}Fe-$\sigma_o(n,2n)$ are those of Ref. [13].

The role of the law of angular momentum conservation in the (n,2n) reaction has been discussed by many authors. In particular, in the publications given in Ref. [14] which analysed the soft part of the experimental neutron emission spectra, the conclusion was drawn that the probability of emission of a second neutron in the (n,2n) reaction is less than it should be from simply taking into account energy conservation laws. The authors of Ref. [14] made a qualitative analysis showing that the reduced probability of neutron emission may be caused by angular momentum conservation. Since the neutron emitted in the first reaction cascade transfers a small amount of energy, on average, and therefore a small momentum, the first residual nucleus has a

large angular momentum and since the second neutron also transfers a small momentum, the second residual nucleus should remain in a state with high spin. Hence, transitions should take place mainly at levels with high spin and the probability of the population of states with low spin should be considerably reduced.

Figure 2 shows the results of theoretical calculations of the probability of population in the reaction (n,2n) for nine levels of the residual ^{55}Fe nucleus, including the ground state. It is evident that it is mainly levels with high spin that are populated and this confirms the qualitative arguments put forward above. In Fig. 3, σ_o(n,2n) (transfer to the ground state of the ^{55}Fe nucleus) is compared with the experimental data in Ref. [13], which agree with our calculations only at energies of 14 and 22 MeV, the energy dependence of the curve differing qualitatively.

Analysis of the reaction cross-sections using the Hauser-Feshbach formula enables the competition of the processes (n,xnγ) and [n,(x+1)n] to be studied properly. Figure 4 shows the calculated neutron emission spectra at initial energies of 12, 13, 15 and 18 MeV, as well as the results of calculations which do not allow for competition of the (n,n',γ) channel. Similar calculations of the excitation functions of the (n,2n) reaction with and without allowance for γ competition are shown in Fig. 5. The greatest effect when the γ-quanta emission channel is included is observed close to the (n,2n) reaction threshold; here, even the shape of the neutron emission spectra changes in the soft part. When the initial neutron energy is sufficiently higher than the threshold (several MeV), the effect of γ-quanta competition is small. Figure 6 shows the effect of γ-quanta competition on neutron emission in the fourth cascade of the ^{165}Ho (α,4n) reaction when substantially greater angular momentum is contributed to the compound nucleus.

The excitation functions cannot be described equally satisfactorily for all the reactions examined by means of the level density parameters from the list in Ref. [7] (Figs 7-10). A consistently better description of experimental excitation functions of the (n,p) reaction is obtained by using the parameters from Ref. [8] which, for the residual nuclei in the channels with proton emission, give a higher level density. Hence these calculations support the similar conclusion drawn earlier in Ref. [5].

The following conclusions can be drawn from a comparison of the calculations with the existing experimental data:

1. The generally accepted models (statistical, optical and pre-equilibrium) satisfactorily describe the excitation functions of reactions affected by various incident particles and satisfactorily reproduce both the shape of the curves and the absolute cross-section.

2. In the region of residual nuclei excitation energies which are high enough for a statistical approach to describe the level density (where the energy of incident particles is several megaelectronvolts above the reaction threshold), the results of calculations using Weisskopf's evaporation model and the Hauser-Feshbach theory agree. In the near-threshold region of the reaction, where a small number of levels are excited and prohibitions significantly affect the quantum mechanical transitions due to allowance for the laws of conservation of angular momentum and parity of the states, the Weisskopf model does not work as well.

3. This paper confirms the discrepancy which we found earlier [5], i.e. the need to choose level density parameters from different systematics in order to describe different reaction channels for nuclei of intermediate mass. The discrepancy stems from the fact that the description of the excitation functions of the (n,xn) and (p,xn) reactions is obtained using the level density parameters taken from Ref. [7]; but in order to reproduce the energy dependence of the (n,p) reaction cross-section, it is necessary to use the level density parameters from Ref. [8].

The reason for this phenomenon is not clear, although we can point to some factors which may cause it:

(a) The Fermi-gas model used to describe the density of excited states gives only a certain approximation to the actual dependence of the nuclear level density on the excitation energy and on the parameter (N-Z) where N and Z are, respectively, the number of neutrons and the number of protons in the nucleus;

(b) In the actual calculations using the statistical theory, the coefficients T(E,U 0) from the optical model are used as transmission coefficients T(E,U), dependent on the energy of the emitted particles E and the excitation energy of the residual nucleus U. Strictly speaking, these coefficients should differ, particularly in the region of low particle energy.

Consequently, a description based on the statistical theory of reaction cross-sections with emission of neutrons and of charged particles will differ since, in the region of low energies, the transmission coefficients for charged particles is insignificantly small due to the effect of Coulomb potential. At the same time, there is a lack of certainty in the calculations of transmission coefficients using the optical model at low scattered particle energies;

(c) In the calculations two types of model are used, the statistical and the exiton, which have been obtained in various physical theories explaining the process. In both models there are parameters which correlate because of the fact that during the experiments the processes described by various models are not separated. Thus there always remains some uncertainty in the choice of these model parameters due to the impossibility of accurately separating the contributions made by the different processes to the experimental results.

REFERENCES

[1] HAUSER, W., FESHBACH, H., Phys. Rev., 1952, v.87, p.366; MOLDAUER, P.A., Rev. Mod. Phys., 1964, v.36, p.1079.

[2] GRIFFIN, J., Phys. Rev. Letters, 1966, v.17, p.478; BLANN, M., Ibid., 1968, v.21, p.1357.

[3] BLANN, M., Phys. Rev., 1978, v.17, p.1871.

[4] STENGL, O.G., UHL, M., VONACH, H., Nucl. Phys., 1977, v. A 290, N 1, p.109.

[5] BYCHKOV, V.M., PASHCHENKO, A.B., Preprint FEhI-699, Obninsk (1976); BYCHKOV, V.M., PLYASKIN, N.I., In: Nejtronnaya Fizika (Neutron physics) (Proc. Fourth All-Union Conference on Neutron Physics, Kiev, 18-22 April 1977) Moscow TsNIIatominform 2 (1977) 84); BYCHKOV, V.M., PASHCHENKO, A.B., FEDOROV, C.V., Preprint FEhI-1217, Obninsk (1981).

[6] UHL, M., STROHMAIER, B., Report IRK - 76/01. Institut für Radium-forschung und Kernphysik. Vienna, 1976.

[7] DILD, W., SCHANTL, W., VONACH, H., UHL, M., Level density parameters for the back-shifted Fermi gas in the mass range 40<A<250. Nucl. Phys., 1973, v. A 217, p.269.

[8] HUIZENGA, J.R., IGO, G., Theoretical reaction cross-sections for alpha-particles with an optical model. Ibid., 1962, v.29 (3), p.462.

[9] PLYASKIN, V.I., TRYKOVA, V.I., Voprosy atomnoj nauki i tekhniki, Ser. Yad. Konst. 21 (1976) 62.

[10] BRAGA-MARCAZZAN, G.M. et al., Phys. Rev., 1972, v.66, p.1398.

[11] LEDERER, C.M., SHIRLEY, V.S., Table of Isotopes, 7-th ed. New York, 1978.

[12] GOVE, N.B., WAPSTRA, A.H., Nuclear - reaction Q - values, Nucl. Data Tables, 1972, v.11, N 2, p.127.

[13] KORKAL'CHUK, V., PROKOPETS, G.A., HOLMQUIST, V., Yad. Fiz. 120 (1974) 1096; Nucl. Phys. A 307 (1978) 445.

[14] SAL'NIKOV, O.A., LOVCHIKOVA, G.N., KOTEL'NIKOVA, G.V. et al., Vzaimnodejstvie 14-MehV nejtronov c yadrami zheleza, medi i niobiya (Interaction of 14 MeV neutrons with iron, copper and niobium nuclei), Preprint FEhI-216, Obninsk (1970); SALNIKOV, O.A., LOVCHIKOVA, G.N., KOTEL'NIKOVA, G.V. et al., Yad. Fiz. (1970) 1132.

[15] BYCHKOV, V.M., MANOKHIN, V.N., PASHCHENKO, A.B., PLYASKIN, V.I., Secheniya porogovykh reaktsij (n,p), (n,α), (n,2n) (Threshold reaction cross-sections for (n,p), (n,α), (n,2n)), 1, P, Voprosy atomnoj nauki i tekhniki, Ser. Yad. Konst. 1 32 (1979) 27.

[16] MARTIN, G.C., PILGER, R.C., Ir. Absolute cross-section and excitation functions for α-particle-induced reactions of ^{165}Ho, ^{164}Er, ^{166}Er and ^{167}Er, Nucl. Phys., 1966, v.89, p.481.

[17] SAU, J., DEMEYER, A., CHERY, R., Etude expérimentale et analuse des fonctions d'excitation ^{165}Ho(α,xn) et ^{169}Tm(α,xn), Ibid., 1968, v.A 121, p.131.

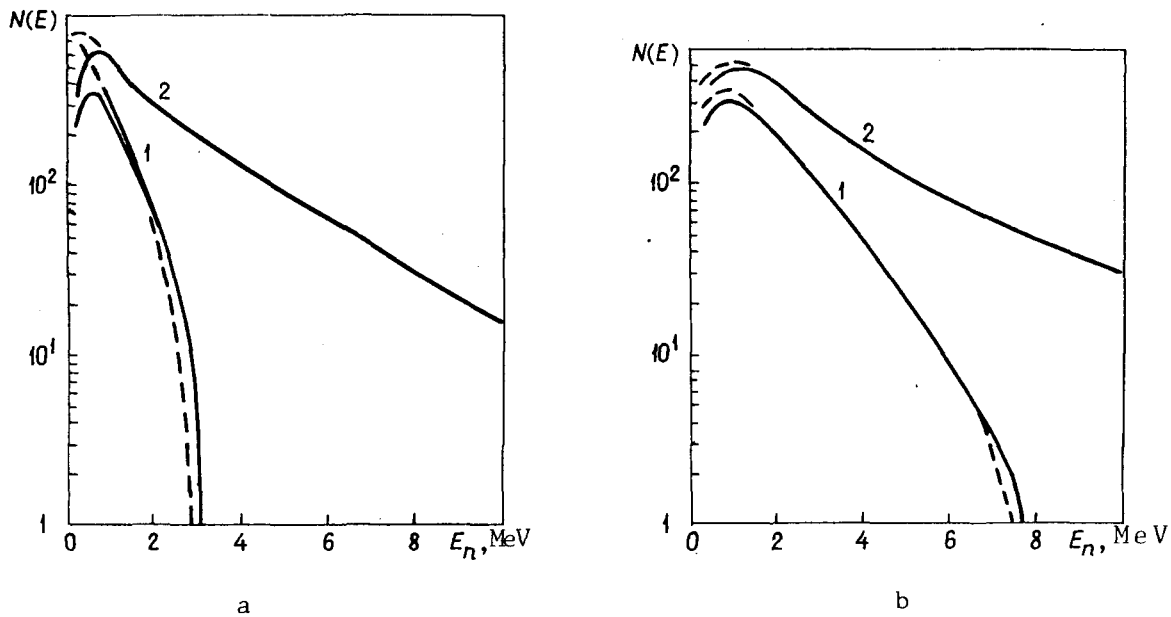

Fig. 1. Results of calculations of neutron emission spectra from the $^{56}Fe(n,2n)$ reaction at (a) 14.5 MeV and (b) 20.6 MeV with nuclear level density parameters from Ref. [7]: - - - - Weisskopf model; ---- Hauser-Feshbach formalism; 1 - secondary neutron spectrum; 2 - total spectrum.

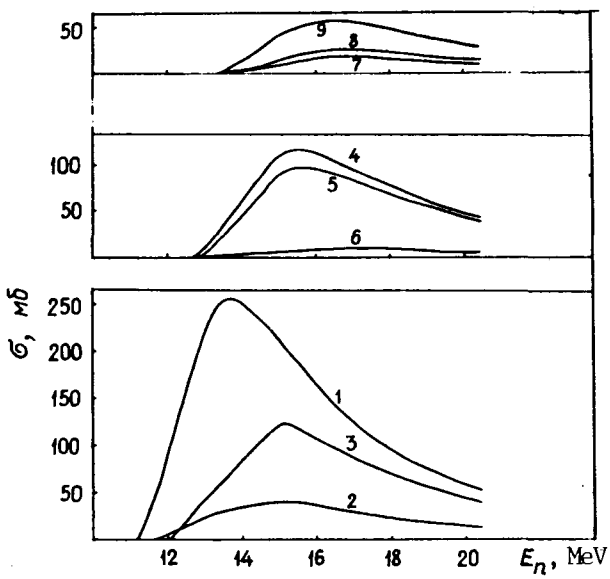

Fig. 2

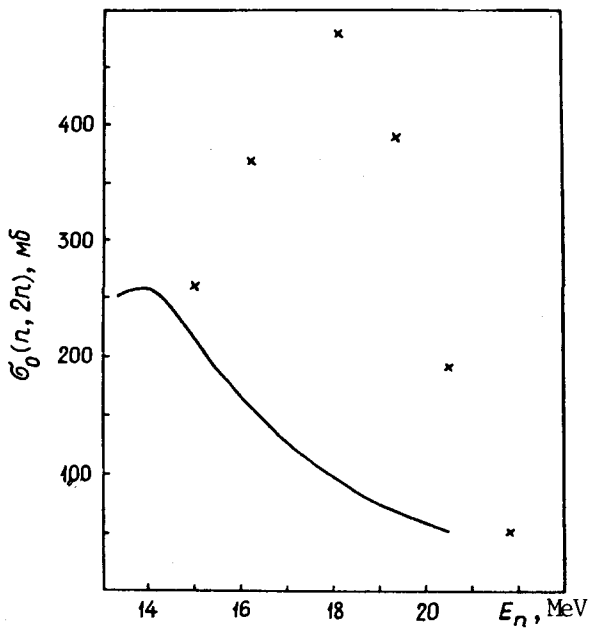

Fig. 3

Fig. 2. Level excitation functions of the residual ^{55}Fe nucleus in the ^{56}Fe(n,2n)^{55}Fe reaction: 1 - 0($I^{\pi} = 3/2^-$); 2 - 0.411($I^{\pi} = 1/2^-$); 3 - 0.931($I^{\pi} = 5/2^-$); 4 - 1.317($I^{\pi} = 7/2^-$); 5 - 1.408($I^{\pi} = 7/2^-$); 6 - 1.919($I^{\pi} = 1/2^-$); 7 - 2.05($I^{\pi} = 3/2^-$); 8 - 2.144($I^{\pi} = 3/2^-$); 9 - 2.212($I^{\pi} = 9/2^-$).

Fig. 3. Comparison of calculated excitation cross-sections for the ground state of the ^{55}Fe nucleus in the ^{56}Fe(n,2n)^{55}Fe reaction (continuous curve) with data from Ref. [13] (indicated by the crosses).

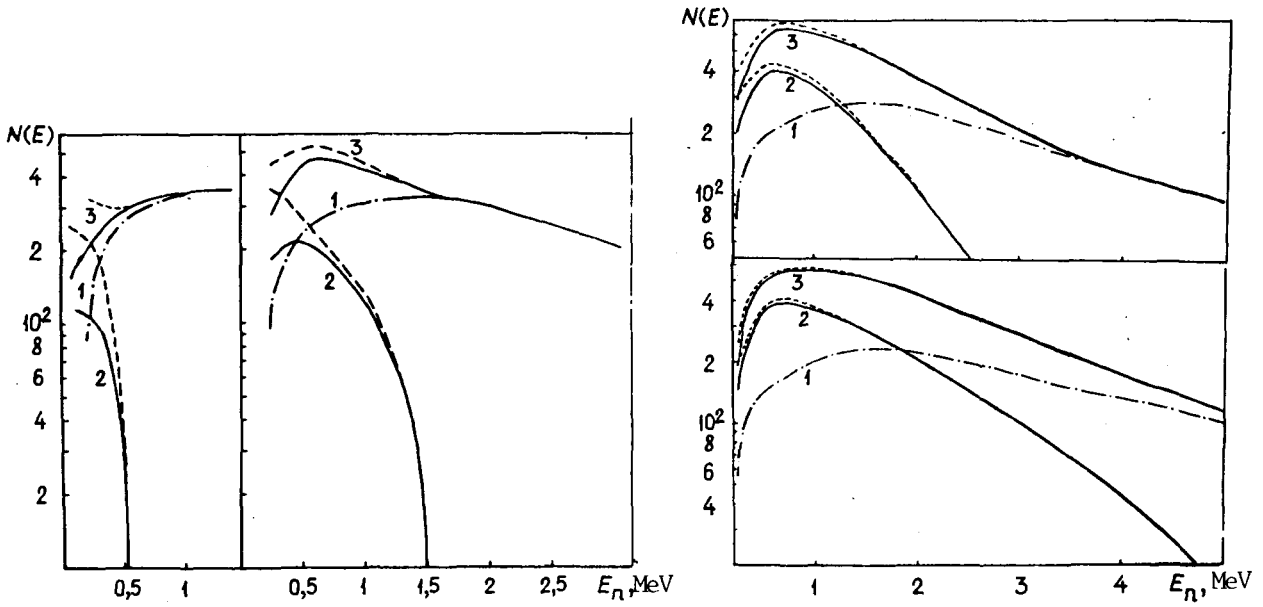

Fig. 4. Effect of competition of the (n,n'γ) channel on the shape of the neutron emission spectrum: (a) at E_n equal to 12 MeV (left) and 13 MeV (right); (b) at E_n equal to 15 MeV (above) and 18 MeV (below). The dotted line shows the calculation without allowing for γ-quanta competition; 1, 2 and 3 are the primary neutron, secondary neutron and total spectra, respectively.

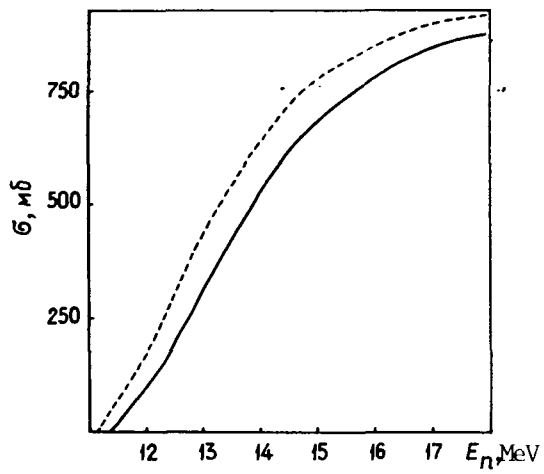

Fig. 5. The effect of γ-quanta competition on the excitation function of the $^{56}Fe(n,2n)^{55}Fe$ reaction (the dotted line does not allow for competition of the γ channel).

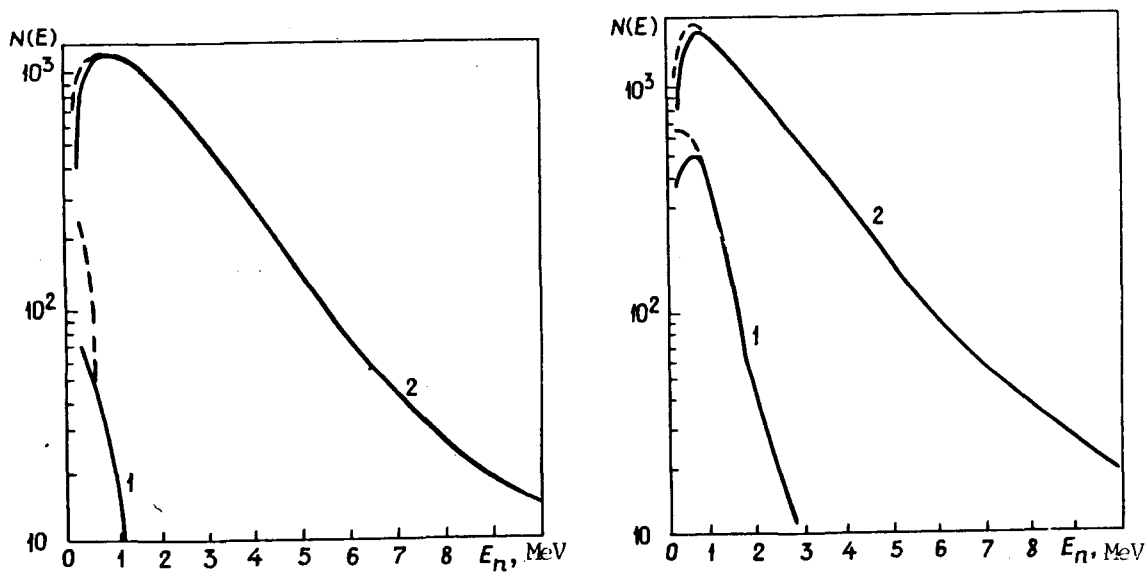

Fig. 6. The effect of competition of the (α,3n,γ) channel on the shape of the neutron emission spectrum in the $^{165}Ho(\alpha,4n)^{165}Tm$ reaction: (a) when E_α = 36 MeV; (b) when E_α = 40 MeV; 1 and 2 are the fourth neutron spectrum and total spectrum, respectively.

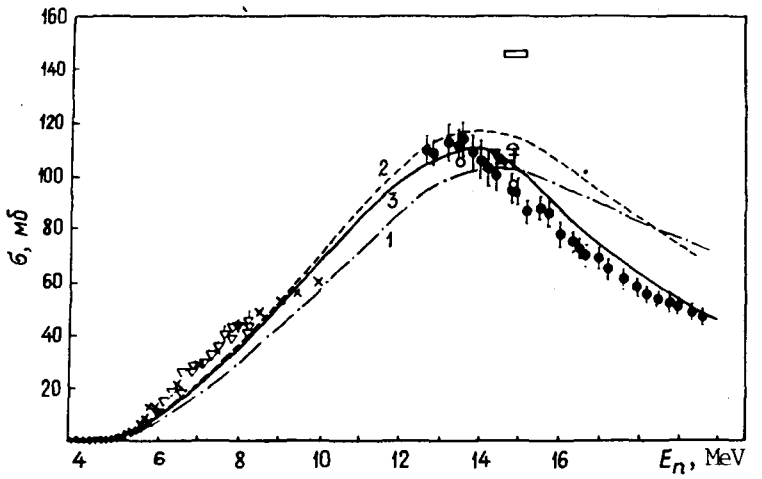

Fig. 7. Excitation functions of the $^{56}Fe(n,p)^{56}Mn$ reaction. Experimental data taken from Ref. [15]. Calculations: 1 uses the STAPRE program with parameters from Ref. [7] and FM coefficient = 670; 2 is taken from Ref. [8] with FM = 670; 3 is taken from Ref. [8] with FM = 1330.

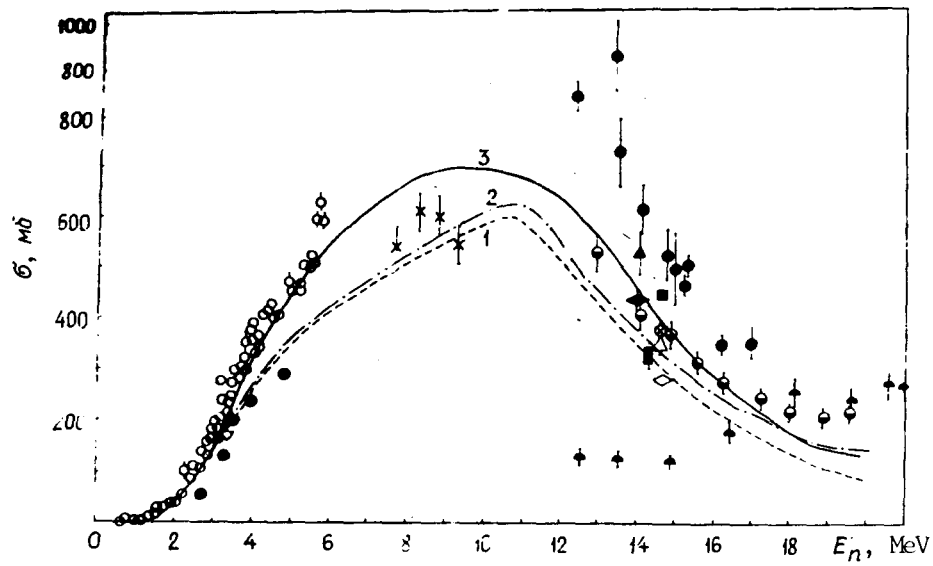

Fig. 8. Excitation functions of the $^{58}Ni(n,p)^{58}Co$ reaction. Experimental data from Ref. [15]. Calculations: 1 - using the STAPRE program with parameters taken from Ref. [7] with FM = 750; 2 - the same with FM = 670; 3 is taken from Ref. [8] with FM = 670.

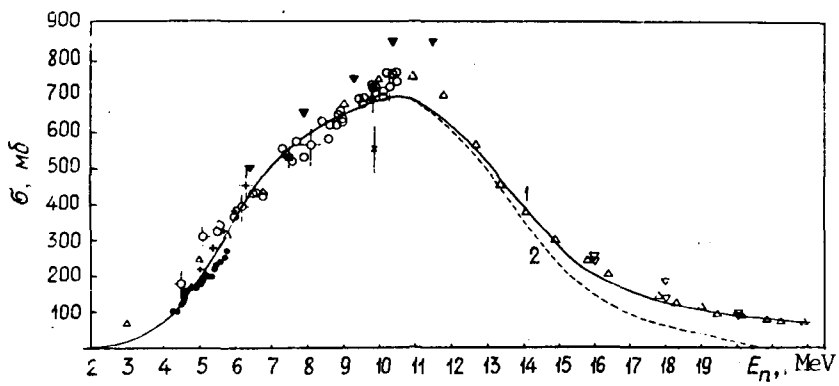

Fig. 9. Excitation functions of the $^{65}Cu(p,n)^{65}Zn$ reaction. Calculations: 1 - using the STAPRE program with parameters from Ref. [7] with allowance for pre-equilibrium neutron emission (FM = 320); 2 - the same without allowance for emission (FM = 0).

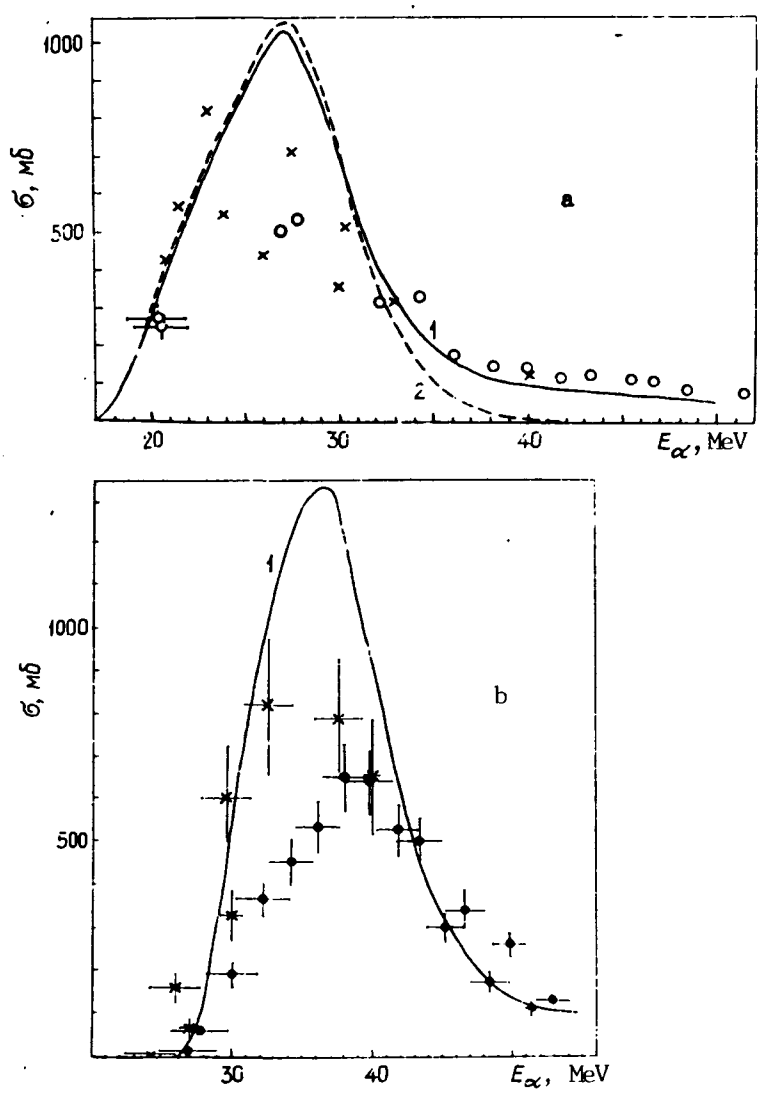

Fig. 10. Excitation functions of the reactions (a) ^{165}Ho(α2n)^{167}Tm and (b) ^{165}Ho(α3n)^{166}Tm. The experimental data are taken from Ref. [16] (x) and from Ref. [17] (●,o). Calculations: 1 - using the STAPRE program with parameters taken from Ref. [7] and allowing for pre-equilibrium emission (FM = 1500); 2 - the same without allowance for emission (FM = 0).

UDC 539.125.5.17

ELASTIC AND INELASTIC SCATTERING CROSS-SECTIONS FOR ^{6}Li AND ^{7}Li NUCLEI AT AN INITIAL ENERGY OF 8.9 MeV

G. Ferch, D. Shmidt, D. Zeliger, T. Shtrail'*/, G.N. Lovchikova and A.M. Trufanov

The study of neutron scattering by lithium isotopes is very relevant to nuclear fusion research since both isotopes produce tritium when bombarded with neutrons. In the case of ^{7}Li, the tritium obtained is associated with an inelastic neutron scattering emission. For this reason it is also very relevant to study the neutron yield channels and to determine the tritium yield directly. However, the results of measurements of integral inelastic scattering cross-sections obtained by various authors differ by 10-60% [1-8]. There is only one publication [3] which makes a systematic study of cross-sections over the primary neutron energy range of 7-14 MeV. The majority of papers published present only partial cross-sections corresponding to elastic and inelastic scattering at low-level excitation. Data on double differential cross-sections, corresponding to the continuous part of the neutron spectra, have been published in Refs [1,4-7], but the measurements given in them at various threshold energies are difficult to compare and constitute more an estimate of the cross-section of this part of the spectrum. Reference 1 deserves particular attention since there the measurements are made at the comparatively low threshold energy of 0.3 MeV. In the present paper, partial elastic and inelastic scattering cross-sections are obtained for ^{6}Li and ^{7}Li isotopes at an initial neutron energy of 8.9 MeV.

Experiment. The measurements were made on an EhGP-10-1 tandem accelerator in the Central Institute for Nuclear Research (Rossendorf GDR). The neutron source was provided by the $D(d,n)^{3}He$ reaction using a gas deuterium target [9]. During operation of the accelerator in a pulsed regime, the neutron flux strength amounted to 10^{8} neutrons/(s.sr). The neutron spectrum of the (d,d) reaction at the specified neutron energy has been studied in detail and is described in Ref. [10]. The neutrons were recorded using a multi-system consisting of eight detectors [11]. The flight path was about 3 m, and the time resolution about 3 ns. The geometrical dimensions and mass of the samples studied are given in Table 1.

---

*/ Technical University (Dresden GDR).

The efficiency of the monitor (a small stilbene crystal was used as a scintillator) and the detectors (NE-213 with an FEhU-63 photomultiplier) was determined from measured spectra of prompt neutrons from spontaneous ^{252}Cf fission [12]. The thresholds of the neutron detectors were about 1 MeV. The energy of the incident neutrons was controlled by the neutron channels corresponding to specific excited states of the residual nucleus in the $^{12}C(n,n')$ reaction.

The neutron spectra were processed by means of the ASYUAR program [13]. Corrections for the effects of multiple scattering, attenuation and the geometry, which were not more than 10%, were introduced on the basis of a KORTUR program [14].

Results of measurements. The partial cross-sections obtained for $^{6}Li(n,n_o)$, $^{6}Li(n,n_1)$, $^{7}Li(n,n_o + n_1)$ and $^{7}Li(n,n_2)$ reactions are given in Tables 2 and 3.

The insufficient energy resolution of the spectrometer prevented us from separating the group of elastically scattered neutrons from the group of inelastically scattered neutrons corresponding to the ^{7}Li level excitation at 0.478 MeV.

Most of the results agree reasonably well with data from other authors [3,6]. However, there is a significant difference between the partial inelastic scattering cross-section for the $^{7}Li(n,n_2)$ reaction, which is 82 ± 20 mb, and the integral cross-section of the same group according to the data in Ref. [3], which is 213 ± 8 mb, and those of Ref. [6], which is 116 ± 11 mb. One of the possible reasons for the difference in the data may be the use of deuterons as bombarding particles. Analysis of the spectrum of the primary neutrons from the target shows that apart from the neutrons of the (d,d) reaction, there is an admixture of neutrons from the $^{12}C(d,n)$ and $^{16}O(d,n)$ reactions. In the case of the $^{7}Li(n,n_2)$ reaction, it is difficult to separate the group of inelastically scattered neutrons n_2 from the group of elastically scattered neutrons due to the presence of neutrons from the $^{16}O(d,n)$ reaction in the direct flux. Although the two groups of neutrons have been separated by means of a program [10], the division is not very accurate. The highest estimate of integral cross-section corresponding to excitation of the n_2 state with 4.63 MeV without spearation of the specified neutron energy is (113 ± 12) mb. The analysis shows that using the (d,d) reaction to measure elastically scattered neutrons

requires careful analysis of all the measured spectra including both the primary and secondary neutrons. This may explain the difference between the data in Ref. [3] in which the (d,d) reaction was also used as a neutron source and the data in Ref. [6] and this paper. The agreement observed, within the limits of experimental error, for the elastic scattering cross-section together with the unresolved component of inelastic scattering neutrons (0.478 MeV), as given by different authors, justifies the supposition made regarding the possible reasons for differences in the data for the σn_2 cross-section.

REFERENCES

[1] Lisowski P.W., Auchampaugh G.F., Drake D.M. e.a. Cross-sections for neutron-induced, neutron-producing reactions in ^{6}Li and ^{7}Li at 5,96 and 9,83 MeV. - Report LA-8342. Los-Alamos, 1980.

[2] FERCH, G., SHMIDT, D., ZELIGER, D. et al., Secheniya uprugovo rasseyaniya nejtronov na yaderakh ^{6}Li i ^{7}Li v oblasti nachal'noj ehnergii 7-10 MehV (Elastic and inelastic scattering neutron cross-sections for ^{6}Li and ^{7}Li at initial energies of 7-10 MeV), In Voprosy atomnoj nauki i tekhniki Ser. Yad. Konst. 1 45 (1982) 7.

[3] Hogue H.H., Von Behren P.L., Glasgow D.W. e.a. Elastic and inelastic scattering of 7 to 14 MeV neutrons from Lithium-6 and Lithium-7. - Nucl. Sci. and Engng, 1979, v.69, p.22-29.

[4] Hopkins J. C., Drake D.M., Conde H. Elastic and inelastic scattering of fast neutrons from ^{6}Li and ^{7}Li. - Nucl. Phys., 1968, v.A107, p.139-152.

[5] Batchelor R., Towle I.H. The interactions of neutrons with ^{6}Li and ^{7}Li between 1,5 and 7,5 MeV. - Nucl.Phys., 1963, v.47, p.385-407.

[6] BIRYUKOV, N.S., ZHURAVLEV, B.V., KORNILOV, N.V. et al., Rasseyanie nejtronov s ehnergiej 9.1 $\pm$ 0.2 MehV yadrami ^{7}Li (Neutron scattering at 9.1 $\pm$ 0.2 MeV for ^{7}Li nuclei), Atom. ehnerg. 43 (1977) 176.

[7] Cookson I.A., Dandy D., Hopkins J.C. Scattering of 10 MeV neutrons by ^{6}Li and ^{7}Li. - Nucl. Phys., 1967, v.A91, p.273-291.

[8] Drake D.M. e.a. Report BNL-NCS-29426. Brookhaven, 1981, p.72.

[9] Mittag S., Pilz W., Smidt D. e.a. Kernenergie, 1979, v.7, p.237.

[10] Smidt D., Meaclorus I. e.a. AN4/NDM-9, 1974.

[11] Eckstein P., Helfer H., Katzmer D. e.a. A multi-angle detector system for fast neutron time-of-flight spectroscopy. - Nucl. Instrum. and Methods, 1980, v.169, p.533-538.

[12] Adel-Fawzy M., Förtsch H., Mittag S. e.a. Kernenergie, 1981, v.24, p.107.

[13] Schmidt D. e.a. Report INDC (GDR)-18/L. Vienna, 1982.

[14] Engelbrecht C.A. Nucl. Instrum. and Methods , 1971, v.93, p.103-107.

Table 1

Characteristics of lithium samples

Isotope	Mass g	Height of sample, cm	Internal diameter cm	External diameter cm	Isotope content %
^{6}Li	8,89	3,0	3,0	I,0	90,I
^{7}Li	9,98	3,0	3,0	I,0	with a four-fold ^{6}Li depletion

Table 2

Differential and integral cross-sections for the $^{6}Li(n,n')$ reaction, mb/sr

Θ cms (centre of mass system) degrees	σ_{n_0}, mb/sr	Θ cms degrees	σ_{n_1}, mb/sr (Q = -2.18 MeV)
23,3	492±30	23,9	I2,9±I,5
46,2	22I±I2	47,3	I3,9±I,6
68,4	56,2±4,2	69,9	I0,I±I,9
89,5	I6,9±2,9	9I,3	7,3±I,0
I09,5	2I,I±2,4	III,3	8,0±I,6
I28,4	I5,8±3,2	I29,9	3,7±I,2
I46,2	I5,7±2,I	I47,3	4,9±0,8
I63,3	2I,0±2,2	I63,9	7,7±I,4
σ_{int} = 1205 ± 50 mb		σ_{int} = 127 ± 10 mb	

Table 3

Differential and integral cross-sections for the $^{7}Li(n,n')$ reaction, mb/sr

Θcms degrees	$\sigma_{n_0 + n_1'}$ mb/sr	Θcms degrees	σ_{n_2}, mb/cr (Q = -4.63 MeV)
22,8	562±32	24,4	I0,6±2,2
45,3	264±I6	48,3	7,4±2,0
67,2	75±6,3	7I,2	6,8±I,6
88,I	33±3,6	92,8	6,5±I,I
I08,I	4I,4±3,4	II2,8	5,4±I,6
I27,2	28,9±3,5	I3I,2	7,3±4,2
I45,3	30,3±2,8	I48,3	4,6±2,I
I62,8	32,0±2,7		
σ_{int} = 1485 ± 65 mb		σ_{int} = 82 ± 20 mb	

UDC 539.17.015

DIFFERENTIAL CROSS-SECTIONS FOR NEUTRON SCATTERING BY Fe NUCLEI OVER THE 0.1-0.8 MeV ENERGY RANGE

A.A. Sarkisov, I.N. Martem'yanov and A.M. Boguslovskij

Studying the characteristics of the interactions of neutrons with nuclei in the resonant energy range is very relevant both to nuclear physics and to solving practical problems. Apart from the integral characteristics of the neutron field which are traditionally studied, increasing attention is being given to its differential characteristics, including a study of differential scattering cross-sections, which contain valuable information about the nature of neutron/nuclei interactions, the mechanism of the neutron reaction process and the structure of nuclei. In addition, these characteristics assist in solving the transport equation and in determining the nature of angular dependence of the neutron flux in reactor and radiation shielding calculations. Therefore, in order to determine the nature of neutron angular distributions more reliably, efforts must be made to improve the accuracy of cross-section determination, to investigate cross-sections at less commonly studied energies and to reduce the angular intervals when making measurements.

To this end, the differential cross-sections of neutrons scattered by iron nuclei (the element most widely used in construction and shielding materials in industrial nuclear facilities) were studied experimentally over the 0.1-0.8 MeV energy range. Although the interaction of neutrons with Fe nuclei has been studied fairly thoroughly, there is a general lack of data on neutron angular distributions in iron at energies lower than 0.35 MeV, and at higher energies there are considerable disparities in the results of different experiments.

Precision measurements for studying the characteristics of neutron/nuclei interaction are generally made with charged particle accelerators (protons and deuterons), which excite T(p,n), Li(p,n), D(d,n) reactions and produce monoenergetic neutrons with energies lower than 14 MeV. The accelerators make it possible to vary the energy of the charged particles and hence that of the neutrons over a wide range. In addition, experiments have shown that the use of spectrally-sensitive detectors, spectrometers with electronic separation of neutrons and γ-quanta as well as collimators for shielding the source-detector system and reducing the background effects of neutrons in "good" geometrical conditions, means that nuclear reactors may be used as neutron sources.

The design of the experimental facility (Fig. 1) is based on the principle of a central geometry, the main feature of which is that the neutron beam emerges through a collimating assembly. The studies were conducted in the horizontal channel 2 of the IR-100 research reactor, the characteristics of which are given in Ref. [1]. The collimators 1, 4, 5 and 7 were used to shape the neutron beam, to position the iron shaping filters and to shield the detection units 8 from background neutrons and scattered γ-quanta (6 indicates the lead screen; 9, the scatterers consisting of the elements studied, 10, the neutron 'trap'). A stilbene (30 x 30 mm) scintillation counter with a (n-γ) separation and pulsed γ-quanta discrimination system was used as a detector. The energy threshold of the facility was 0.1 MeV at near 100% effective separation of the neutrons from the γ-quanta. The level of γ-quanta discrimination was 10^{-4}.

The energy resolution (as a percentage) of the single-crystal spectrometer is described very well in the energy range examined by the relationship $\eta = A/\sqrt{E_n}$, where A is a constant (between 10 and 20) which depends on the quality and dimensions of the stilbene crystal, and may also be limited by the resolution of the FEhU photomultiplier itself (by selecting a crystal and FEhU with the highest quantum yield we can obtain A = 12); E_n is the neutron energy in MeV.

This paper gives direct measurements of the neutron fluxes from which we calculated the cross-sections of interest to us. In simplified form, the differential scattering cross-sections may be determined by the expression:

$$\sigma_s(\theta) = \left(N_i^{\theta} - N_i^{0}\right)\left(r^2/N_0 n S\right), \qquad (1)$$

where N_i^{θ} is the calculation rate when the detector is in position for observing the neutrons scattered at an angle, when the scatterer is present; N_i^{0} is the background calculation rate with the detector in the same position but without the scatterer; $N_i = N_i^{\theta} - N_i^{0}$ is the counting rate with subtraction of the background; N_0 is the counting rate when the detector is in the position usually occupied by the scatterer; r is the distance between the scatterer and the detector; n is the total number of nuclei in the scatterer; S is the aperture of the detector. θ, n, S and r in Eq. (1) are measured just before the experiment and are only monitored during it. N_i^{θ}, N_i^{0} and N_0 are measured directly. In view of the statistical

explained by the interference between the incident and scattered waves. Apart from the clearent peak forwards, there is an absence of fluctuation in the region of the angles $\theta > \pi/2$ and displacement to this region of minima in the angular distribution. As the neutron energy increases, the angular distribution becomes increasingly anisotropic.

The method of iron resonance filters used in this paper made it possible to remove the resonance neutrons from the beam and to create optimum conditions for describing the angular distributions by the optical model. At present, great attention is being paid to studying the direct and collective effects and the application for angular distribution analysis of the generalized optical model. However, in view of the characteristic behaviour of the angular distributions over the energy range examined, one of the variants of the spherical optical model may be used. In the calculations the Bjorklund-Fernbach local optical potential [3] was used with the following fixed parameters of the optical model: V_o = 52 MeV; W_{CJ} = (6 + 0.75 E) MeV; a = 0.65 fm*/; = 0.98 fm; $_o$ = 1.25 fm. As Fig. 3 shows, the experiment and the calculations agree reasonably well.

In order to study the mechanism by which neutrons interact with Fe nuclei, evaluations were made of the difference between elastically scattered cross-sections for unfiltered neutron beams and filtered neutron beams passing through iron filters (Fig. 4). Curves 1 for each energy value represents the neutron angular distributions for the unfiltered beam [cross-section $\sigma_i(\theta)$], curves 2 is the filtered beam [scattering cross-section $\sigma_i^f(\theta)$] and curves 3 is the different neutron angular distributions [scattering cross-sections $\Delta\sigma_i(\theta) = \sigma_i(\theta) - \sigma_i^f(\theta)$].

The difference $\Delta\sigma_i(\theta)$ is very clearly diffractional. The angles symmetrical with respect to $\theta = \pi/2$ differ by a factor of more than 1.5 (i.e. clearly beyond the limits of all the experimental errors). The experimental data acquire definite physical meaning if the average neutron cross-section in the intervals between resonances and the average cross-section in the resonance region are regarded as constituent parts of the average elastic scattering cross-section. In this case, each scattering experiment may be regarded as the result of two experiments on the elastic scattering of neutrons from two beams with identical effective energies but

---

*/ 1 femtometre (instead of the obsolete fermi) = 10^{-15} m.

nature of particle interaction, accuracy in determining the differential cross-section depends not only on the accuracy of the first group of values but also on the statistical reliability of N_i and N_o. Since $N_o \gg N_i$, statistical error needs considering only when determining N_i.

To obtain the true value of $\sigma_i(\theta)$ in Eq. (1), corrections are made for multiple scattering in the filter and the scatterer; these are determined by simulation of the experiment using the Monte Carlo method and the neutron data in Ref. [2]. ^{56}Fe (98%) nuclei were studied. Hollow cylinders with transparency along the diameter of about 0.9 were used as scatterers and plates with transparency of about 0.1 served as filters. The measurements were made repeatedly and at 10 angles which represented the cosines from -0.9 to +0.9 at an interval of 0.2. The frequent repetition of the operation was intended to enable the spread of data from separate experiments in the series to be evaluated. The large number of angles yielded information about the differential cross-sections in the form of neutron angular distribtuions for nine fixed energy levels: 0.13, 0.18, 0.24, 0.34, 0.41, 0.5, 0.59, 0.69 and 0.80 MeV (Fig. 2).

The experimental results were approximated by Legendre polynomials. The conventional expression

$$\sigma_s(\mu) = \frac{1}{4\pi} \sum_{\ell=0}^{N} B_\ell P_\ell(\mu), \qquad (2)$$

was taken as its basis, where μ is the cosine of the scattering angle in the laboratory system of co-ordinates; B_ℓ are the expansion coefficients of the experimental angular distributions by Legendre polynomials; $P_\ell(\mu)$ is the Legendre polynomial of the order ℓ. The expansion coefficients were determined by the least squares method. The optimum number of polynomials needed to describe the experimental data with a degree of accuracy in keeping with the experimental errors, was obtained using Gauss' criterion. The approximation curves are represented in Fig. 2 by continuous lines. As the calculations showed, over the energy range examined, the angular distributions can be satisfactorily approximated by second-order Legendre polynomials.

Regularities are observed in the behaviour of the angular distributions of neutrons over the energy range examined. As the energy increases, scattering forwards becomes increasingly predominant. This maximum can be

different spectra. This is the same as if the differential scattering cross-sections corresponded to two nuclei of very different dimensions.

The results of this experiment have certain similarities with those of Ref. [4], but the behaviour of the different angular distributions emphasizes the resonance nature of neutron scattering by iron nuclei. The neutron flux penetrating the beam after multiple scattering in the filter does not exceed 1% of the total flux in the filtered beam. The statistical errors in the experimental data are given in Fig. 2. The error in determining the cross-sections for iron in the experiment is about 5%.

The results obtained experimentally for the differential scattering cross-sections supplement the data system on the interaction of neutrons with iron nuclei in the little studied 0.1–0.8 MeV region of resonance energy.

REFERENCES

[1] KONSTANTINOV, L.V., MARTEM'YANOV, I.N., NIKOLAEV, V.A. et al., Ehksperimental'no izuchenie kharakteristik issledovatel'skogo reaktora IR-100 (Experimental study of the characteristics of the IR-100 research reactor), At. Ehnerg. 29 (1970) 453.

[2] GARBER, D., KINSEY, R., Neutron Cross-Sections, BNL-325 (1976) v. 2.

[3] BJORKLUND, F., FERNBACH, S., SHERMON, M., Local potential and parameters of the optical model for interpretation of the elastic neutron scattering, Phys. Rev., (1958) v. 109, p. 1295.

[4] MOROZ, V.M., ZUBOV, Yu.G., LEBEDEVA, N.S., O dvukh mekhanizmakh uprugogo rasseyaniya v opticheskoj modeli yadra (Two mechanisms of elastic scattering in the optical model of the nucleus) Yad. Fiz. 17 4 (1973) 134.

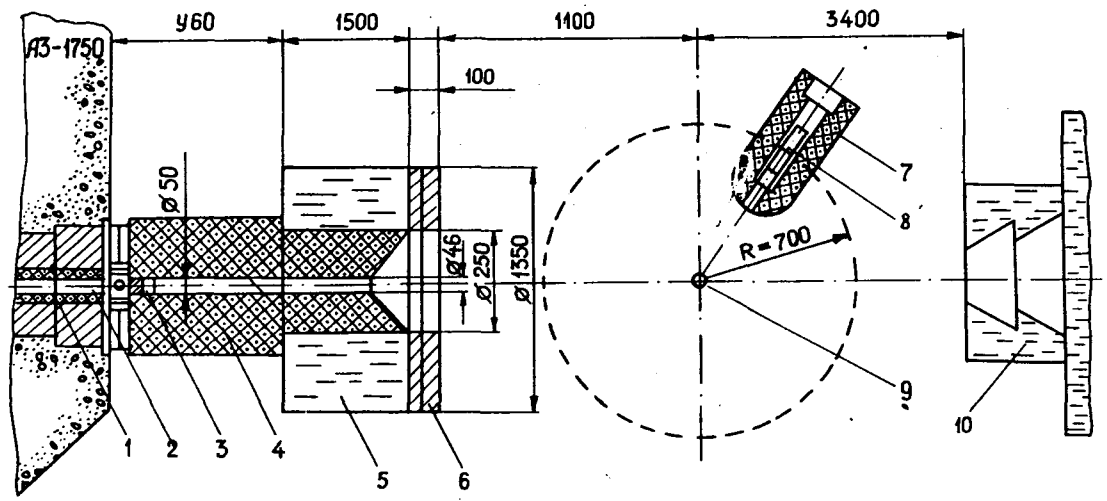

Fig. 1. Diagram of the experimental facility and geometry of the experiment.

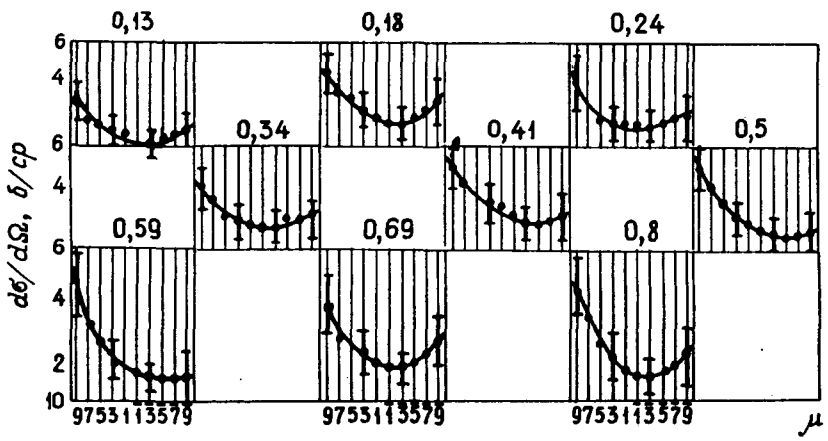

Fig. 2. Angular distributions of neutrons scattered by iron nuclei and their approximation using Legendre polynomials.

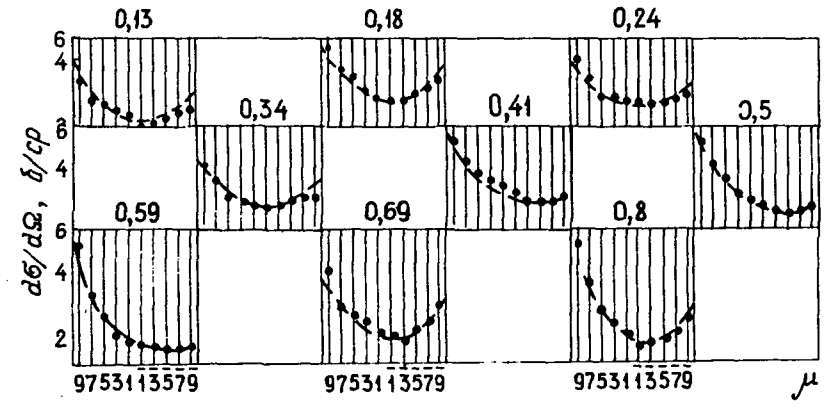

Fig. 3. Angular distributions of neutrons scattered by nuclei:
• - the experiment; ---- - calculation from the optical model.

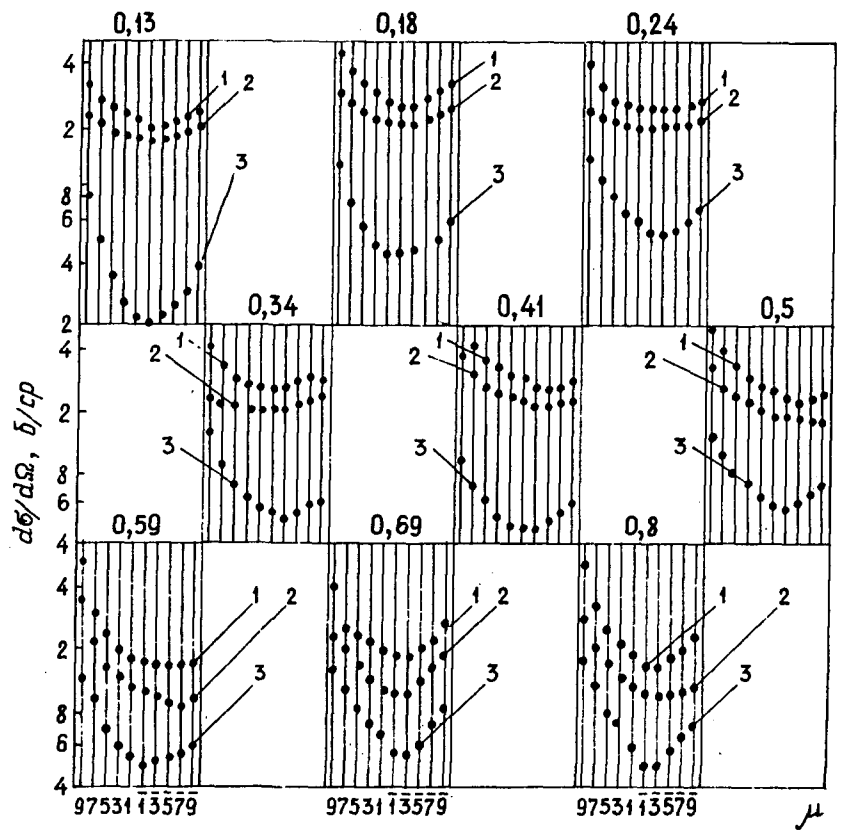

Fig. 4. Angular distributions of non-filtered neutrons and neutrons filtered with iron filters.

UDC 539.125.5.17

INVESTIGATION OF EMISSION NEUTRON SPECTRA FROM ^{235}U AT INCIDENT NEUTRON ENERGY OF 4.9 MeV

G.N. Lovchikova, O.A. Sal'nikov, S.P. Somakov,
S.Eh. Sukhikh, A.V. Polyakov, A.M. Trufanov

The measurement of the differential and integral characteristics of the interaction of fast neutrons with the nuclei of fissile elements has great practical and scientific value. The importance of these data for fast critical assembly and reactor calculations has been pointed out repeatedly in required nuclear data lists [1,2]. Experimental studies of these processes are also important in order to understand the mechanism of nuclear reactions and the structure of nuclei. So far, only a small amount of experimental material has been acquired. The aim of this paper is to measure the spectrum of secondary neutrons produced by the bombardment of ^{235}U with 4.9 MeV neutrons.

Experiment. The ^{235}U emission neutron spectra were investigated by the spectrometer time-of-flight technique described by Trufanov and co-workers [3]. The monoenergetic neutron source was a gas tritium target which was bombarded with a pulsed proton beam in a EhGp-IOM accelerator. The design and characteristics of the target are given in the paper of Fetisov et al. [4]. The frequency of the proton pulses was 5 MHz, the width about 1 ns and the mean proton current on the target was 1 μA. The energy of neutrons emitted from the target was 4.9 ± 0.06 MeV. The spectrometer channel width in the measurements was 0.431 ns, the integral non-linearity was 0.4%, the time resolution was 3 ns at half the peak height of prompt γ-quanta, which at neutron energies of 1.3 and 5 MeV corresponded to an energy resolution of 40, 200 and 440 keV.

The 90% enriched ^{235}U sample (scatterer) in the shape of a hollow cylinder with an external diameter of 45 mm, internal diameter of 40 mm and height of 50 mm contained 1215 moles of ^{235}U nuclei. The scatterer was placed at an angle of 0^{o} to the proton beam at a distance of 17 cm from the centre of the gas tritium target.

The neutrons from the scatterer were recorded by a scintillation detector over a flight path of 200 cm. The detector consisted of a stilbene crystal with a diameter of 6.3 cm and height of 3.9 cm scanned by an FEhU-30

photomultiplier. A (n-γ)-separation system in the form of an electric signal was used which meant that the γ-quanta background could be largely suppressed. The detector was placed in a shield of lithium hydride, paraffin and polyethylene [3] to suppress the background of neutrons scattered by the walls of the room and neutrons emitted directly from the target. The shield, moving in an arc with its centre in the place where the sample was positioned, could be placed at different angles to the neutron beam incident to the scatterer. The neutron threshold was 0.5 MeV.

The monitor for the neutron flux incident on the sample was a scintillation detector, similar to the main one but with a smaller stilbene crystal (diameter 4.0 cm and height 2.0 cm) and without a shield. The detector measured the time spectrum of the neutrons from the target. The monitor was shielded from the γ-quanta flux by a 5 cm thick lead shield placed 350 cm from the target at an angle of 50° to the proton beam. The neutron yield from the target was monitored by a wave counter placed 300 cm from the target at an angle of 90° to the proton beam. In addition, the total charge (number) of protons incident on the target was monitored by a current integrator.

Measurements and processing. In this paper, measurements were made of the emission neutron spectra for ^{235}U at angles of 30°, 45°, 60°, 90°, 120°, 150° at an incident neutron energy of 4.9 MeV. In order to reduce the effect of operational instability of the accelerator and electronic equipment on the measurement results, the spectra for each angle were measured 20 times every 20 minutes. The operational stability of the accelerator and electronic units was monitored by the shape and position of the neutron peak of the monitor, by the shape of the spectrum of the direct neutron flux and the stability of the position of the peaks of the direct neutron beam and prompt γ-quanta of detector in the monitoring channel and the main detector, respectively.

The measurement procedure involved determining the spectra with the scatterer (effect with background) and determining the background with a fixed number of protons incident on the target. At the same time, the monitor measured the neutron spectrum of the target. The effect with background and the background without tritium in the target were also determined. The contribution to the spectra of emission neutrons produced in the sample during measurements with an evacuated target was small (units of channel counts) and was regarded in the processing as part of the constant background.

The spectrum of neutrons scattered by hydrogen nuclei at an angle of 45^{o} to the incident neutron beam was measured in order to determine the absolute values. Here the scatterer used was a polyethylene CH_2 cylinder (diameter 10 mm and height 50 mm) with 3.11×10^{23} nuclei. The spectrum of neutrons from the target at an angle of 0^{o} was measured in order to determine the shape of the peak of elastically scattered neutrons.

The neutron detector recording efficiency was determined experimentally by measuring the neutron spectrum of spontaneous ^{252}Cf fission, the shape of which was satisfactorily described by a Maxwellian distribution with the parameter T = 1.42 MeV. In these measurements, the scatterer was replaced by a fission chamber with a ^{252}Cf layer. The detector efficiency was also calculated on the basis of a program [5] for a stilbene crystal. In the energy region higher than 8 MeV, a calculation curve was used since the accuracy of experimental determination of efficiency was inadequate. Figure 1 shows the dependence of the detector efficiency on the neutron energy. The difference between the experimental and calculated data at low energies was determined by the effect of the γ-quanta suppression system on efficiency. The correlated and uncorrelated backgrounds were calculated from the spectral measurements. The first background component was normalized with respect to the area below the peak on the monitor spectrum. The second component was determined from the average number of channel counts in the energy region near 20 MeV where there were virtually no fission neutrons produced by the pulsed neutron beam.

The recorded spectra are shown in Fig. 2. In the separation of the peak of elastically scattered neutrons allowance was made for the shape of the direct neutron flux from the target to the detector. For this purpose the straight peak was used to determine the boundaries of the regions of the recorded spectrum where the contribution of elastically scattered neutrons became less than the statistical spread and between these regions parabolic interpolation of the spectrum into the region of the elastic peak was performed. The emission neutron time spectrum thus obtained was converted to the energy scale with allowance for the detector efficiency.

Apart from statistical error, the main components of the total error in the emission spectra measured were error in determining the detector efficiency, uncertainty in separating the elastic scattering process, mistakes involved in the final sample and detector measurements and error in determining the position of the γ-peak. Calculation of the error in determining

efficiency on the basis of the ^{252}Cf fission neutron spectrum gives an error of 4-6% in detector efficiency. The error involved in subtracting the elastic peak in the 3.8-5.5 MeV region gives an error of nearly 11%. The statistical error is 1-2% in the region up to 3.8 MeV and increases from 5 to 20% in the region above 5.5 MeV. The error in determining the position of the γ-quanta peak (of the 0.5 channel) and the uncertainty in the flight path gives an error of 1% in the spectrum. The absolute values of the spectra were derived by normalization to the (n,p)-scattering cross-section [6]. At the same time, the spectra measured with the polyethylene sample were corrected for neutron flux attenuation and multiple scattering. Corrections were not made for attenuation and multiple scattering in the ^{235}U sample since estimates made in Refs [7 and 8] show that they can be disregarded for samples similar to those used in this paper.

Measurement results. The neutron emission spectra obtained for angles of 30°, 45°, 60°, 90°, 120° and 150° were integrated over the angles and energies. At an incident neutron energy of 4.9 MeV, apart from elastic interaction of $\sigma_{e\ell}$, an important contribution to the total cross-section, σ_t, is made by inelastic scattering, $\sigma_{n,n'}$, and fission $\sigma_{n,f}$ [9]. Therefore, the value of the integrated spectra obtained may be regarded as consisting of two components: $N = \sigma_{n,n'} + \bar{\nu}_p \sigma_{n,f}$, where $\bar{\nu}_p$ is the average number of prompt fission neutrons emitted in one fission event [10]. In this paper we obtained a value of $N = 5.45 \pm 0.44$ b.

The values $\bar{\nu}_p = 3.03 \pm 0.06$ [10] and $\sigma_{n,f} = 1.07 \pm 0.01$ b [11] were taken to derive the integral inelastic scattering cross-section, $\sigma_{n,n'}$. As a result, the inelastic scattering cross-section for ^{235}U nuclei at a neutron energy of 4.9 MeV, was found to be 2.21 ± 0.44 b which, as can be seen from Fig. 3, agrees satisfactorily with the measurement results [12-14]. The inelastically scattered neutrons and prompt fission neutrons contribute to the neutron spectra for separate angles and the integral neutron spectrum in the energy region below 4.9 MeV. Above 4.9 MeV, only fission neutrons contribute.

In order to obtain the double-differential inelastic scattering cross-sections $\partial^2\sigma/\partial E\partial\Omega$, the spectrum of prompt fission neutrons in the form of the Maxwellian distribution $AE^{1/2}\exp(-E/T)$ was subtracted from the spectra measured at various angles. It was assumed that the angular dependence of the shape of the spectrum and the absolute value of the fission neutron emission, within the accuracy of the experiment, was small [16]. The normalizing constant of

the Maxwellian distribution was determined as

$$A = \frac{1}{4\pi} \frac{2\bar{\nu}_p \sigma_{n,f}}{\pi^{1/2} T^{3/2}} ,$$

where $\sigma_{n,f}$ = 1.07 b is the ^{235}U fission cross-section at an incident neutron energy of 4.9 MeV [11]; T = 1.38 MeV is the temperature of the fission neutron spectrum. The temperature was calculated from the relationship $\bar{E}_n = 3T/2$ at an average energy of the fission neutron spectra of $\bar{E}_n$ = 2.09 MeV as obtained by Batchelor and Wyld [15] for fission spectra at an incident neutron energy of 7 MeV. Figure 4 shows the energy spectrum of emission neutrons measured at an angle of 90° to the primary neutron beam, the Maxwellian distribution and the spectrum of inelastically scattered neutrons. The discrepancy between the fission spectrum in our measurements and the Maxwellian distribution in the region above 4.5 MeV is due to the difficulties in separating the peak of elastically scattered neutrons and the background not connected with the source. The double-differential inelastic scattering cross-sections obtained were integrated over the angles and the energies and, as a result, the integral inelastic scattering cross-section was found to be 2.88 $\pm$ 0.51 b. Within the limits of experimental error, this agrees with the value obtained from the integral emission neutron spectrum which was 2.21 $\pm$ 0.44 b.

REFERENCES

[1] WRENDA 76/77. INDC (SEC)-55/URSF. Vienna, 1976.

[2] WRENDA 79/80. INDC (SEC)-73/URSF. Vienna, 1979.

[3] TRUFANOV, A.M., NESTERENKO, V.S., FETISOV, N.I. et al., Pribory i tekhnika ehksperimenta (Experimental apparatus and techniques), 2 (1979) 50.

[4] FETISOV, N.I., SIMAKOV, S.P., TRUFANOV, A.M. et al., Ibid. 6 (1980) 22.

[5] CHULKOV, L.V., Preprint IAEh-2594, 1975.

[6] HORSLEY, A., Nucl. Data, 1966, v.A 2, N 3, p.243.

[7] SAL'NIKOV, O.A., FETISOV, N.I., LOVCHIKOVA, G.N. et al., AN SSSR Ser. Fiz. XXXII (1968) 653.

[8] JOHANSSON, P.I., HOMLQVIST, B., Nucl. Sci. and Engng, 1979, v.52, p.695.

[9] SCHUSTER, S.H., HOWERTON, R.J., J. Nucl. Energy, 1964, v.A/B 18, p.125.

[10] SAVIN, M.V., KHOKHLOV, Yu.A., ZAMYATIN, Yu.S. et al., Nuclear Data for Reactors, Vienna, IAEA 2 (1970) 157.

[11] CZIRR, J.B., SIDHU, G.S., Nucl. Sci. and Engng, 1975, v.57, p.18.

[12] BETHE, H.A., BEYSTER, J.R., CARTER, R.E., Report LA-1939, 1955.

[13] BARIBA, V.Ya., ZHURAVLEV, B.V., KORNILOV, N.V. et al., Atomnaya Ehnergiya 43 4 (1977) 266.

[14] BERTIN, A., BOIS, R., FREHAUT, J., Trans. Amer. Nucl. Soc., 1975, v.22, p.664.

[15] BATCHELOR, R., WYLD, K., Report AWRE-O, 55/69, 1969.

[16] KNITTER, H.-H., ISLAM, M.M., COPPOLA, M., Z. Physik, 1972, v. 257, p.108.

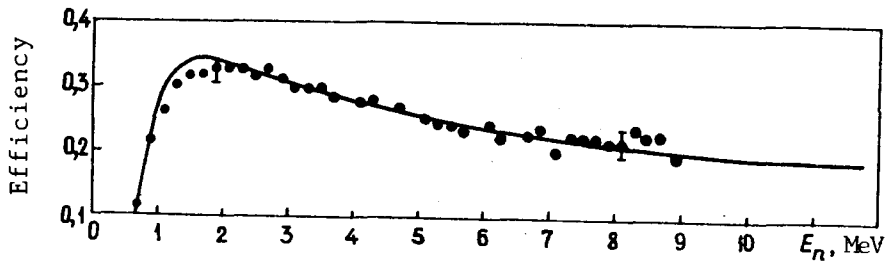

Fig. 1. Detector efficiency in recording neutrons over ^{252}Cf fission neutron spectra (•) and calculation by program [5] (curve).

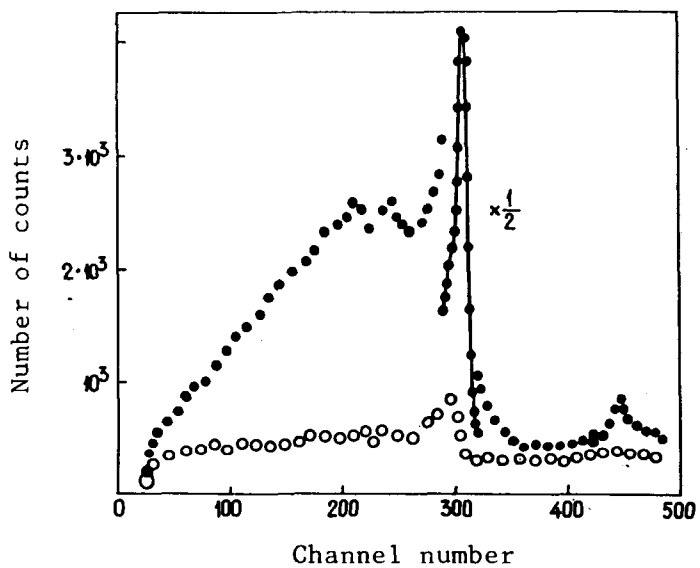

Fig. 2. Recorded spectra with ^{235}U sample (•) and without it (o).

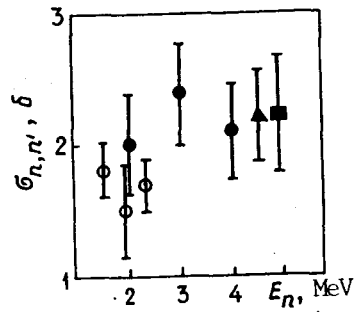

Fig. 3. Inelastic scattering cross-sections at various energies of incident neutrons measured by authors in the list of references: ▲ - [15]; ● - [13]; O - [14]; ■ - ours.

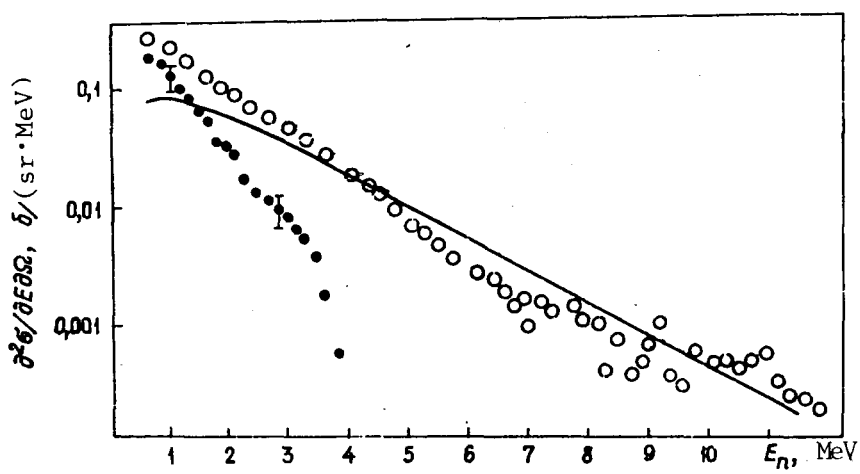

Fig. 4. Emission neutron spectra at an angle of 90°: O - total; ● - from the (n,n') reaction; —— - fission neutron spectrum in the form of a Maxwellian distribution with T = 1.38 MeV.

UDC 621.170.013

ANALYSIS OF TRANSMISSION EXPERIMENTS FOR ^{238}U IN THE UNRESOLVED RESONANCE REGION

A.A. Van'kov, L.S. Gosteva, V.F. Ukraintsev

It is generally thought that the ^{238}U nucleus has been relatively well studied from the point of view of neutron interaction constants. Nevertheless, even in this area, there is no uniformity in evaluation methods or in the optimum choice of mean resonance parameters for obtaining group constants in the region of unresolved resonances. For example, in the paper of Abayyan et al. [1] it is concluded from analysis of resolved resonances that either p-resonances are not subject to Porter-Thomas statistics or nearly half of the p-resonances are transmitted and a definite spin dependence of the level densities is observed. The authors of Ref. [1] incline to the second alternative and use this theoretically unfounded premise in the calculation model for ^{238}U group constants (taking the mean distance between s-resonances to be $\bar{D}_{1/2^+} = 20.8$ eV, $\bar{D}_{1/2^-} = 13.2$ eV). Hence it follows that the radiation width of the p-resonances has to be half as large as the s-resonances (in order to conserve the generally accepted radiation strength function). The conclusion is also drawn that the transmission function measurements are not accurate enough to be used to define the calculated self-shielding resonance factors more accurately. As we shall see later, this conclusion is erroneous. The majority of other studies on the evaluation of mean resonance parameters are based on more consistent theoretical concepts of the model for calculating neutron cross-sections, although irregular dependence of certain parameters (neutron strength functions) on neutron energy is allowed [2]. At the same time, it is clear that the choice of calculation model and evaluated mean resonance parameters plays a decisive role in the determination of group constants. Experimentally observed mean cross-sections are of course decisive although distortions caused by the finite thickness of the sample seriously impede direct evaluation of true mean cross-sections in the region of unresolved resonances. Accurate knowledge of the total cross-section is particularly important in evaluating mean resonance parameters. However, in order to determine this precisely, all the transmission functions including

those for the largest thicknesses must be measured. Resonance self-shielding factors cannot be analysed without recourse to experimental material on transmission functions. Transmission functions in the form:

$$T(n)=\frac{1}{\Delta u}\int_{\Delta u}\exp\left[-\sigma_t(u)n\right]du,$$

can be measured the most reliably and directly determine the resonance self-shielding factors of the total cross-section. However, knowledge of these functions also considerably improves the accuracy of the self-shielding resonances factors of the reaction cross-sections. This paper seeks to investigate the role of similar experiments in improving the accuracy of mean resonance parameters and thereby of group constants in the region of unresolved resonances, using ^{238}U as an example.

Short discussion of experimental work. In the work described in Ref. [3], carried out by members of the staff of the Institute of Physics and Energetics (Obninsk) the Joint Institute for Nuclear Research (Dubna), on the IBR reactor time-of-flight spectrometer, the neutron transmission functions were measured for metallic depleted ^{238}U samples. The measurements were made over a wide range of neutron energies (E_n < 100 keV) and sample thicknesses (0.5-200 mm) at three temperatures (the temperature of liquid nitrogen, room temperature and 1040 K). Later, the group of authors of Ref. [3] repeated the separate measurement cycles several times with improved recording equipment using ^3He counters and better background conditions (at the level of 1-2%).

A series of similar transmission experiments at three temperatures has also been performed on an RPI linear accelerator (time-of-flight spectrometer with E_n < 100 keV), also with the use of metallic depleted uranium samples but over a range of smaller thicknesses (about 1.5-13 mm) [4]. In this paper, the self-indication functions were measured during radiative capture. However, the lack of information about background, to which such measurements are particularly sensitive, and also possible distortions in the results due to the finite thickness of the sample-indicator, seriously diminish the value of these data. In attempting to analyse them, we found serious contradictions.

In the Institute of Physics and Energetics, measurements have also been made of transmission and self-indication functions (by the group led by V.N. Kononov [5]). A lithium target in an electrostatic generator was used as a neutron source. The measurements were made over a neutron

energy range of about 10-100 keV for the first part of sample thicknesses. Since these experiments are continuing in order to improve the reliability of the results, we will not analyse them in this paper.

Lastly, the results of measuring the temperature dependence of transmission have been published [6]. Samples of uranium oxide were used which meant that high temperatures could be reached. These results agree qualitatively with the results of measuring the temperature dependence of transmission (the Doppler effect) in the paper of Van'kov et al. [3]. Nevertheless, problems concerning the theoretical interpretation of the experiments with the oxide samples prevented us from making a quantitative analysis of the data of Haate and Sowerby [6]. Due to the thinness of the heated sample observed by Byonn et al. [4], the Doppler effect is regrettably comparatively small. Therefore we were not particularly interested in this part of the data in Ref. [4].

Thus the experimental material on transmission functions for ^{238}U which proved to be suitable for use in theoretical analysis, consisted of the data of the group working in Dubna on the spectrometer of the IBR reactor (transmission functions and temperature dependence of transmission for large-thickness samples) and the data of the RPI group (transmission functions). Figure 1 shows the results of these experiments at room temperature.

Conditions of analysis. It was necessary to clarify some of the conditions of analysis which are given below:

1. The choice of the lethargic averaging interval. It is reasonable to assume that the interval must be such that the fluctuation (the probable deviation from the mean as a result of natural resonance statistics) of such quantitites as the mean cross-sections and their resonance self-shielding factors does not exceed the maximum permissible error. Otherwise, the local fluctuation of the observed value will generate spurious dispersion of the mean resonance parameters. Our investigations have shown that the lethargic intervals of the BNAB system in the region of unresolved resonances for ^{238}U only just satisfy this criterion. For example, over the range of 4.65-10 keV, these fluctuations (the mean square deviations) lie within the range of 2-4%.

It is interesting to note that the shape of the distribution of some functionals (for example σ_t) is essentially asymmetrical. For practical purposes, it is convenient to take the intervals of energy groups which are identical to the intervals of the constants system, since the analysis results can immediately be compared with the data tables.

2. Checking the information content of the experiment. Table 1 shows various types of error of a typical transmission curve for ^{238}U in the region of unresolved resonances in the averaging interval $\Delta u = 0.77$. The measurement errors roughly correspond to the experimental conditions [3]. These errors are determined for the most part not by statistical calculation but by the mean square spread for several series of measurements under different conditions. The correlation between the points is evidently small since many independent error factors are involved. The a priori error is obtained using the sensitive coefficients on the assumption that the mean resonance parameters (neutron strength functions s_o and s_1, the mean distance between s-resonances $\bar{D}$ and scattering radius R') have an uncertainty of 15%.

The fluctuational error (due to natural resonance statistics) in the interval selected $\Delta u = 0.77$ is small. The a priori and experimental errors are similar. More precise definition of parameters is expected but it would have been desirable for the experimental error to have been 2-3 times less. Experimental transmissions for thicknesses greater than 64 mm were not analysed since they were measured with a wide open collimator; the possibility of systematic errors is not excluded.

In theory, there is still another type of error affecting optimization - the error in calculating the mean functionals by the Monte-Carlo method. This error is $\sqrt{N}$ times less than the fluctuational error, where N is the number of random sampling of neutron cross-sections in the particular group. A typical value for N is 25, so that this error can be disregarded in these calculations.

The role of experimental transmissions as a function of sample thickness for accurately defining a particular parameter can be predicted by examining the sensitivity pattern of the transmission functions to the parameters. Figure 2 shows the relative sensitivity coefficients of the functions

$$T(n) \equiv T_g(n) = \frac{1}{\langle \sigma_g \rangle} \int \sigma_g(u) \exp[-\sigma_t(u) n] du$$

for the eleventh and twelfth groups, i.e. for the range 4.65-21.5 keV. There is a remarkable similarity of sensitivity behaviour for the functions T(n) and $T_\gamma(n)$. This shows that adding information about $T_\gamma(n)$ to information about T(n) does not essentially change the situation as far as accurate definition of the constants is concerned.

3. The choice of variable parameters. The authors used a standard one-level Breit-Wigner formulism. Generation of the neutron cross-section resonance structure was carried out by the Monte Carlo method in accordance with nuclear level statistics. The calculation method is described in a paper of Bakalov et al. [7]. The s- and p-states were taken into account. The (2j + 1) law for level densities was used. In the tenth group (21.5-46.5 keV), correction was made for the variation in level density that was exponentially dependent on the excitation energy and also for the increase in radiation width required by the theory. The s- and p-neutron reduced strength functions, S_o, S_i, the mean distance between s-resonances $\bar{D}$, the scattering radius R' (identical for s- and p-neutrons and determining the potential cross-section at low energy $\sigma_p = 4\pi R'^2$) were taken as independent parameters. The mean radiation width also varied but had practically no effect on the transmission function.

The authors established that in order to describe the experimental data on group cross-sections and transmission functions in the neutron energy region of 1-46 keV accurately, within the limits of experimental error, a set of parameters could be chosen which did not depend on the neutron energy (accurate to the limits posed by the reservations made regarding group 10) or contradict the evaluations in the region of resolved resonances. However, the best description of transmission functions, including those for the largest thicknesses, is obtained, if one assumes that some reduction in R' is possible at high energies (groups 10 and 11). As is well-known, calculations based on the optical model show that R' decreases monotonically as energy increases. With the coupled channel method [8], we obtained a variation in R' of 1.4% for a variation in E_n of 1-10 keV and of 4% for a variation in E_n of 10-46 keV. Therefore, in the optimization process, a difference of 1.5% in R' was allowed during transition from the tenth to eleventh group. We did not feel that it was necessary to introduce the energy dependence of the reduced strength functions.

4. The optimization method. The Bayes optimization method was used [9]. The a priori parameter errors, the experimental errors, discrepancies between calculations and experiments and the sensitivity coefficients matrix had to be specified. The errors have been discussed above. Displacements of the parameters and their posteriori errors were obtained (co-variation matrix). The group constants and their a posteriori errors were calculated from the new parameters.

5. The method of calculating the group constants. The group constants were obtained from the calculated distribution functions of the total cross-section $P(\sigma_t)$ and the correlation functions of partial cross-sections with the total cross-section $\sigma_x(\sigma_t)$. The role of the calculation scale along the σ_t axis was studied. The scale chosen ensured high accuracy in calculating the functionals (at least as good as 1%). The general formula for calculating the functional $\langle M(\sigma_t,\sigma_x)\rangle$ has the form:

$$\langle M(\sigma_t,\sigma_x)\rangle = \int_0^\infty M[\sigma_t,\sigma_x(\sigma_t)]P(\sigma_t)d\sigma_t$$

The example of the $P(\sigma_t)$ and $\sigma_x(\sigma_t)$ functions is shown in Fig. 3.

Analysis results. The quality of the description of the experimental points by means of calculation curves using the optimized parameters can be seen from Fig. 1. The parameter evaluations are given in Table 2. The a posteriori evaluation obtained does not contradict the existing evaluations of mean resonance parameters in the region of resolved resonances. It should be noted that in the evaluation obtained, there is a distinct negative correlation of the a posteriori evaluations S_1 and R'.

Table 1 shows the a posteriori error in the transmission function (an error obtained on the basis of the co-variation matrix of the optimized parameters). It is evident that it is close to the maximum limit of fluctuational error, below which accurate determination has no physical meaning.

A comparison of the evaluations of group cross-sections $\langle\sigma_t\rangle$ and $\langle\sigma_\gamma\rangle$ with BNAB-78 data [1] is given in Table 3. It will be seen that the latter are systematically lower by 0.5-1 b for $\langle\sigma_t\rangle$ and by 5-8% for $\langle\sigma_\gamma\rangle$ (groups 11 and 12). The $\langle\sigma_\gamma\rangle$ error is generally determined by $\bar{\Gamma}_\gamma$ which transmission experiments do not make more accurate.

Evaluations of resonance self-shielding factors are given in Table 4. It shows that the a posteriori evaluation is significantly different from the a priori in the direction of an increase in the effect of self-shielding. The error largely depends on the σ_o dilution cross-section. Thus, the a priori error for $f_t(0)$ is 10-20% (depending on the number of the group) and for $f_t(100)$ is 1-4%. The corresponding a posteriori errors are nearly half the size. The a priori errors for $f_\gamma(0)$ are 2-5% and for $f_\gamma(100)$, 0.5-1.5%. The corresponding a posteriori errors are 20-30% less than the a priori errors.

A comparison of the data in Table 4 with the corresponding BNAB-78 data [1], shows the systematic underestimation of the effect of resonance self-shielding in Ref. [1], in comparison with the results of our work. This problem has practical importance since knowledge of the transport cross-section determines the reliability of the calculation of heat release in power reactors and accurate determination of the resonance self-shielding factors of ^{238}U absorption cross-sections is necessary in order to solve the old problem of the difference between the integral data for $\langle\sigma_\gamma\rangle$ and the corresponding microscopic data which demand higher values of $\langle\sigma_\gamma\rangle$.

Conclusion. From analysis of experimental data on transmission in the region of unresolved resonances we obtained an evaluation of the mean resonance parameters which did not contradict the corresponding evaluations from the region of resolved resonances. On the basis of this evaluation, we determined the ^{238}U group constants for the region of unresolved resonances and evaluated the corresponding errors. A comparison was made with data tables.

REFERENCES

[1] ABAGYAN, L.P., BAZAZYANTS, N.O., NIKOLAEV, M.N., TSIBULYA, A.M., Gruppovye konstanty dlya rascheta reaktorov i zashchity [Group constants for reactor and shield calculations] Moscow: Ehnergoizdat, (1981).

[2] **Sowerby M.G., Bee W.J. ^{238}U Unresolved Resonance Parameters. INDC (NDS)-129/GJ, Vienna; IAEA, 1981, p. 136-149.**

[3] VAN'KOV, A.A., GRIGOR'EV, Yu.V., NIKOLAEV, M.N. et al., Temperaturnaya zayisimost' struktury polnogo sechniya ^{238}U [Temperature dependence of the ^{238}U total cross-section structure] In: Nuclear Data for Reactors 1 (1976) 559.

[4] **Ryonn T., Block R.C., Sember T. Temperature dependent transmission measurements of ^{238}U. - In: Proc. Conf. - 720901, 1972, BNL.2, p.1115-1131.**

[5] KONONOV, V.N., POLETAEV, E.D., BOKHOVKO, M.V. et al., Izmerenie faktorov rezonansnoj blokirvki secheniya zakhvata nejtronov dlya ^{238}U [Measurement of resonance blocking factors for ^{238}U neutron radiative capture cross-section] In: Nejtronnaya fizika (Proceedings of the 5th All-Union Conference on Neutron Physics, Kiev, 15-19 September 1980) Part 2. Moscow TsNIIatominform (1980) 276.

[6] **Haste T.I., Sowerby M.G. A study of the temperature dependence of the neutron transmission of uranium dioxide. - Proc. of an Internat. Conf. Nuclear Physic and Nuclear Data. Harwell, sept. 1978, OECD Nuclear Energy Agency, 1978, p.332-336.**

[7] BAKALOV, T., VAN'KOV, A.A., ILCHEV, T. et al., Analiz ehksperimental'nykh dannykh po propuskaniyu nejtronov v oblasti nerazreshennykh rezonansov ^{239}Pu [Analysis of experimental data on neutron transmission in the region of ^{239}Pu unresolved resonances] Soobshcheniye P3-83-51 OIYaI (1982).

[8] IGNATYUK, A.V., LUNEV, V.P., SHORIN, V.S., Raschety sechenij rasseyaniya nejtronov metodom svyazannykh kanalov [Calculations of neutron scattering cross-sections by the coupled channel method]. Voprosy atomnoj nauki i tekhniki. Ser. Yadernye Konstanty. 13 (1974) 59.

[9] VAN'KOV, A.A., Bajesovskiy podkhod v interpretatsii rezultatov fizicheskikh ehksperimentov [The Bayes approach to interpreting the results of physical experiments]. Yadernye Konstanty, Moscow: Atomizdat 16 (1974) 11.

TABLE 1

Typical errors of a transmission function for ^{238}U in the region of unresolved resonances

Error %	Sample thickness n, mm						
	I	2	4	8	I6	32	64
A priori	0,6	I,2	2,2	3,8	7,3	I2	20
Fluctuational	0,2	0,3	0,4	0,7	I,0	I,5	4,0
Experimental (2σ)	I	2	3	4	5	8	I0-20
A posteriori (2σ)	0,3	0,4	0,6	I,0	I,6	2,6	5,2

TABLE 2

Evaluations of mean resonance parameters for ^{238}U

Parameters and their errors	$S_o \times 10^4$	$S_i \times 10^4$	R' fm	$\bar{D}$ eV	$\bar{\Gamma}_\gamma$ MeV
Initial values	I,I0	2,30	9,28	22,9	2I,6
A priori error % (2σ)	I5	I5	I5	I5	I0
Optimized values	I,I4	2,07	9,I3(gr. I0,II) 9,28(gr. I2,I3)	2I,6	2I,6
A posteriori error % (2σ)	8	I0	I,5	I2	I0

TABLE 3

Evaluations of group total cross-section and radiative capture cross-section for ^{238}U, b

Number of Group	E_n, keV	Evaluation				
		a priori	a posteriori		BNAB-78[1]	
		$\langle\sigma_t\rangle$	$\langle\sigma_t\rangle$	$\langle\sigma_\gamma\rangle$	$\langle\sigma_t\rangle$	$\langle\sigma_\gamma\rangle$
I0	2I,5-46,5	I4,2 (8,3%)	I3,9 (2,3%)	0,444	I3,5	0,445
II	I0-2I,5	I5,2 (8,3%)	I5,I (2,8%)	0,630	I4,5	0,597
I2	4,65-I0,0	I6,7 (8,4%)	I7,0 (3,9%)	0,882	I5,9	0,8I4
I3	2,I5-4,65	I9,9 (9,3%)	I9,5 (4,4%)	I,23	I8,9	I,24

TABLE 4

Evaluation of resonance self-shielding total cross-section factors and radiative capture cross-section for σ_o dilution cross-section of 0 and 100 b

Number of Group	E_n, keV	Evaluation							
		a priori				a posteriori			
		$f_t(0)$	$f_t(100)$	$f_\gamma(0)$	$f_\gamma(100)$	$f_t(0)$	$f_t(100)$	$f_\gamma(0)$	$f_\gamma(100)$
I0	2I,5-46,5	0,803	0,968	0,885	0,984	0,682	0,963	0,883	0,983
II	I0-2I,5	0,620	0,92I	0,789	0,962	0,523	0,9I2	0,789	0,96I
I2	4,65-I0,0	0,488	0,845	0,668	0,9I7	0,4I0	0,837	0,652	0,9I0
I3	2,I5-4,65	0,242	0,708	0,487	0,8I4	0,305	0,72I	0,479	0,803

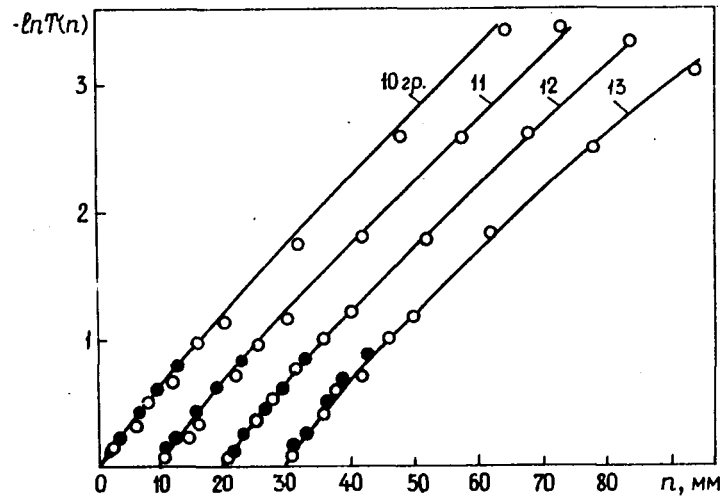

Fig. 1. Results of measurements of transmission functions T(n) for ^{238}U in the neutron energy region of 2.15-46.5 keV (groups 10-13): o - on the IBR spectrometer [3]; • - on the RPI spectrometer [4]. The continuous curve is the calculation from the optimized parameters. The beginning of the counts on the scale n for groups 11-13 are displaced.

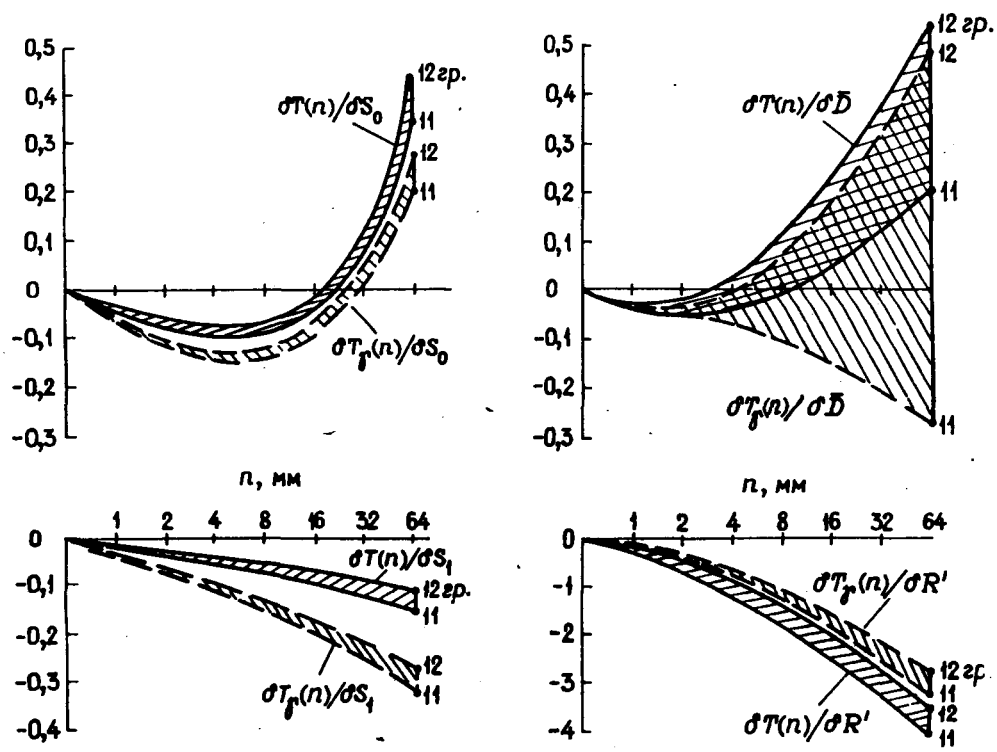

Fig. 2. The sensitivity coefficients for the T(n) and $T_\gamma(n)$ functions relative to the ^{238}U mean resonance parameters.

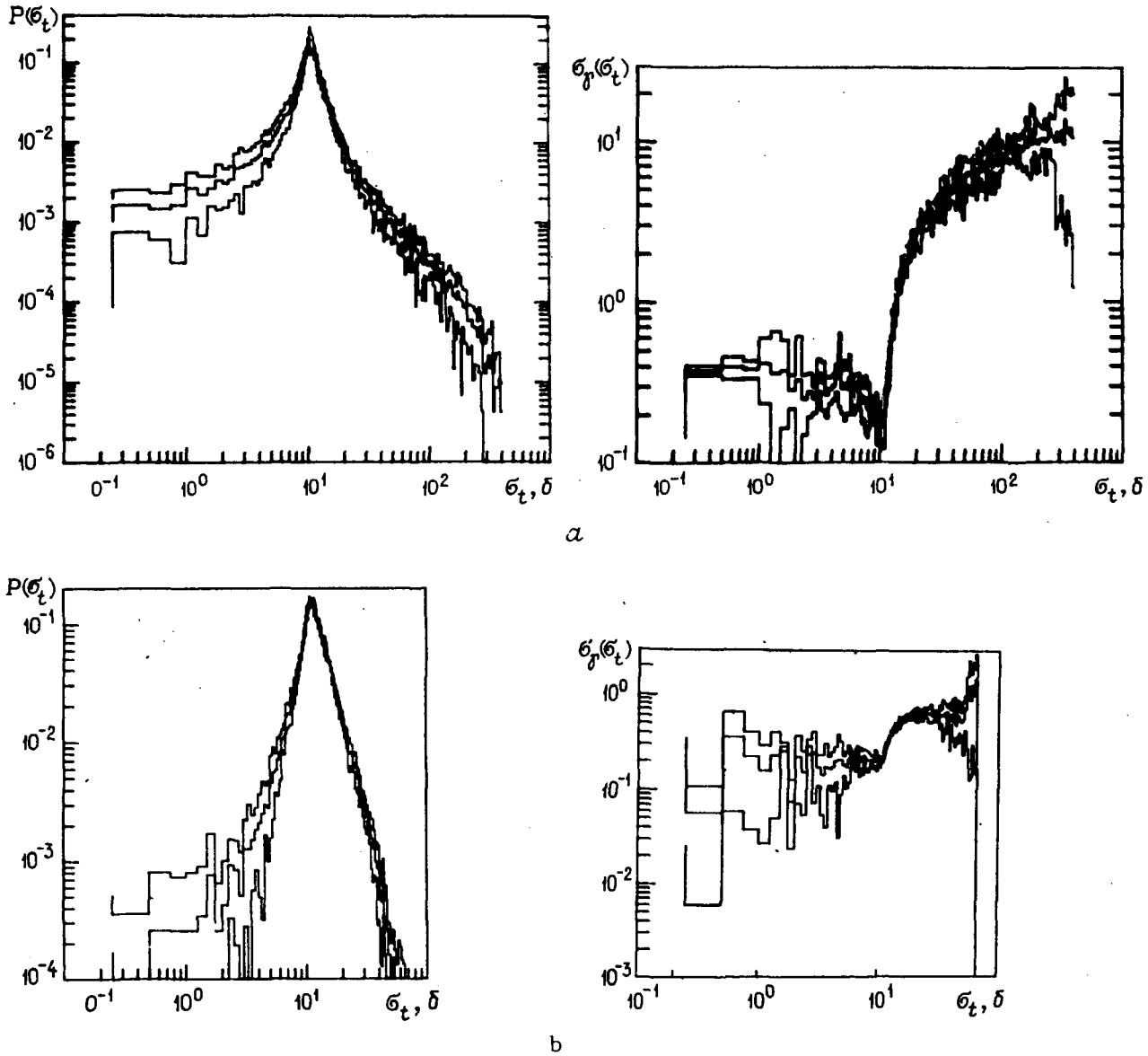

Fig. 3. Distribution $P(\sigma_t)$ and the correlation function $\sigma_\gamma(\sigma_t)$ for ^{238}U over the ranges 1-2.15 keV (a) and 21.5-46.5 keV (b). The upper and lower lines mark the boundaries of the margin of fluctuational error.

UDC 621.170.013

GROUP CONSTANTS AND CHARACTERISTICS OF THE NEUTRON CROSS-SECTION STRUCTURE FOR ^{232}Th, ^{240}Pu AND ^{242}Pu IN THE UNRESOLVED RESONANCE REGION

A.A. Van'kov, S. Toshkov, V.F. Ukraintsev,
Chan Khan' Maj and N. Yaneva

Knowledge of the constants of the isotopes ^{232}Th, ^{240}Pu and ^{242}Pu is important for the development of nuclear power based on the use of fast neutron reactors: these isotopes are components of the raw materials in different fuel cycles. In contrast to ^{238}U, these isotopes have been studied relatively little, particularly with regard to constants in the region of unresolved resonances which is of practical importance. Direct measurement of these constants is extremely difficult due to the strong effects of resonance self-shielding and the "inconveniences" familiar to those carrying out neutron spectrometry experiments over the 1-20 keV energy range. The experimental material on this subject consists of a small number of works which are not always systematized. Thus, in the reference information on nuclear constants [1] there is a lack of data on ^{232}Th and ^{242}Pu and the data on mean cross-sections and resonance self-screening factors for ^{240}Pu are obtained by various methods and are therefore not self-consistent. There are scarcely any measurements on transmission functions for these isotopes mentioned, although they are necessary for analysis of the calculated resonance self-shielding factors. Under these circumstances, the theoretical calculation model plays a very important role in providing us with group constants. In the case of even mass number A isotopes, the situation is made easier by the fact that the influence of inter-resonance interference effects on the mean cross-sections and the cross-section momenta is small and therefore the Breit-Wigner single-level formula may be used. Thus, the problem is one of selecting properly the evaluation of the corresponding mean resonance parameters and developing the theoretical formalism so as to obtain, simultaneously, both the mean cross-sections and the mean characteristics of the neutron cross-section resonance structure (resonance self-shielding factors and so on) based on a simple model. This is the aim of this paper.

Calculation model. The Hauser-Feshbach equation [2] would be sufficient if only the mean cross-sections needed to be calculated. However, in order to calculate what we call the cross-section momenta from which the resonance self-shielding factors are obtained, as well as to calculate the transmission functions (in the case of analysis of transmission experiments), it is necessary to average explicitly the corresponding functionals from the known distributions of nuclear level statistics. This has to be done, furthermore, for each state of the compound nucleus in terms of momentum and parity. For our purposes, it is, in practice, sufficient to take into account the contributions of the s- and p-waves; in this case, there are not so many states as there are for odd nuclei, where the nucleus-target spin is different from zero. At energies below the first level of inelastic scattering, the condition $\overline{\Gamma}_n/\overline{D} \ll 1$ is observed and the known Breit-Wigner equations take the form:

$$\sigma_t(E) = 4\pi\lambda^2 \sum_{J,\pi} g(J)\sin^2\varphi_\ell + 4\pi\lambda^2 \sum_{J,\pi} g(J)\left(\Gamma_n^J/\Gamma^J\right)\left[\Psi(x,\xi)\cos 2\varphi_\ell + X(x,\xi)\sin 2\varphi_\ell\right]; \quad (1)$$

$$\sigma_x(E) = 4\pi\lambda^2 \sum_{J,\pi} g(J)\left[\Gamma_n^J \Gamma_x^J/(\Gamma^J)^2\right]\Psi(x,\xi). \quad (2)$$

Here Ψ and X are the known Doppler functions of the arguments x,ξ[$x=2(E-E_o)/\Gamma$, $\xi=\Gamma/2\Delta$, where Δ is the Doppler width]. The phases of potential scattering ϕ_ℓ are linked to the so-called radii of the R_ℓ scattering, which can be linked to the radius of the nucleus (entrance channel a_c taking into account the contribution of the far levels R_ℓ^∞; $R_\ell = a_c(1 - R_\ell^\infty)$. In the first approximation we can consider that R_o (for s-neutrons) and R_1 (for p-neutrons) are identical and linked to the potential cross-section at low energies: $\sigma_p = 4\pi R_o^2$. The other parameters of the calculation model are strength functions: the neutron S_n and radiation S_γ (the ratio of the corresponding mean widths to the mean distance between levels) in each state. Accurate experiments show the dependence of level density on the total momentum J and slight dependence on the kinetic energy of the neutrons E_n:

$$\rho_J \sim \rho_0\left[(2J+1)/U^2\right]\exp\left\{\sqrt{2aU} + \left[J(J+1)/2\sigma^2\right]\right\},$$

where U is the excitation energy, i.e. the sum of the binding energy for the neutron B_n and the kinetic energy E_n; σ and a are the constant parameters of the level density. Therefore s_o and s_1 emerge as mean resonance parameters (the reduced strength functions of the s- and p-neutrons). The mean radiation width, determining the radiation strength functions, is a further independent

parameter. For heavy nuclei $\bar{\Gamma}_\gamma$ is generally used which is identical in all states since there are no clear experimental or theoretical indications to suggest that $\bar{\Gamma}_\gamma$ is dependent on spin or on parity. The last independent parameter needed for calculating partial cross-sections is the mean distance between s-resonances. There are enough parameters listed to apply Eqs (1) and (2) with allowance for the dependence of the neutron widths on energy by means of the well-known transmission formula v_ℓ.

The energy dependence (the variability) of the mean resonance parameters R_ℓ and S_ℓ is open to discussion. In fact, the optical model (including the model of non-spherical potential with allowance for deformation of the nucleus by the coupled channel method [3]) shows that the dependence of the potential cross-section on the neutron energy is greater than that expressed in Eq. (1). This may justify the choice of lower values for the effective radius R_o in the region of higher energies. A similar dependence may be introduced also for the S_ℓ parameters, although there is often talk of making them free parameters of the energy group in order to fit the mean cross-sections (or transmission) experiments. Such "emancipation" may be regarded, for example, as a means of empirically calculating possible irregularities in the behaviour of the intermediate structure cross-sections or other effects lying outside the scope of our theoretical calculation model. This is actually done in the case of fissile nuclei in view of the more complex physics of the neutron interaction. We believe that this approach is not essential for even nuclei. In our work, the reduced mean resonance parameters are assumed to be constant if corrections for the increase in level density at high energies are disregarded and likewise corrections for some increase in the width of $\bar{\Gamma}_\gamma$ demanded by the theory.

With a set of evaluated mean resonance parameters it is possible to calculate the mean values by averaging over the Porter-Thomas distribution for reduced neutron widths and over the Wigner distribution for the distances between levels. Two methods are possible: numerical integration using some sort of squares and the Monte Carlo generation of the neutron cross-section structure as a function of the neutron energy. As far as laboriousness of the calculations is concerned, there is not much to choose between the two approaches. The authors chose the second method since it proved to have advantages when applied to the simulation of neutron cross-sections in terms

of the multi-level R-matrix formalism. In addition, this particular method can be used for specialized study of the role of functional fluctuations by means of natural nuclear level statistics in the last energy range. Until now, this area has hardly been investigated. An algorithmic description of the simulation of the neutron cross-section structure is contained in Ref. [4]. The number of "random samplings" in each specified group was chosen large enough to ensure that the error in the mean functionals due to statistical analysis did not exceed 2%. All the functionals were calculated on the basis of the distribution density functions for total cross-section $P(\sigma_t)$ and the correlation functions for partial cross-section σ_x with the total - $\sigma_x(\sigma_t)$, which were obtained in the series of "random sampling". The general equation for the functional F has the form:

$$\langle F(\sigma_t, \sigma_x)\rangle = \int_0^\infty F\left[\sigma_t, \sigma_x(\sigma_t)\right] P(\sigma_t)\, d\sigma_t \ . \qquad (3)$$

The choice of calculation scale for numerical integration (3) was studied separately and conditions ensuring its non-dependence on the results with an accuracy of at least 1% were obtained.

Evaluations of mean resonance parameters. One might expect that the properties of heavy even-even isotopes would be close in many respects. In particular, there is no reason for an appreciable difference between the parameters R_ℓ and S_ℓ for these nuclei. This is convincingly demonstrated by the experimental results on total cross-sections, obtained in Ref. [5] for heavy fissile and non-fissile nuclei with A ≈ 232-240 over the range E_n ≈ 0.03-10 MeV. These cross-sections hardly differ from one nucleus to another. This conclusion was confirmed by our calculations using the optical model [3] with optimized parameters describing significant experimental material on total and differential cross-sections [6]. Table 1 gives the calculation results for E_n = 10 keV. In view of the physical difference between the R-matrix and the optical model, it follows that account should be taken of the weak dependence of the parameters determining the characteristics of neutron interaction on the mass number in the region of heavy even nuclei (apart from $\overline{\Gamma}_\gamma$ and $\overline{D}$).

In the various evaluations of the mean resonance parameters there are values determined by analysis of specific experimental data (in the region of resolved and unresolved resonances), usually in isolation from the A-systematics. The various evaluations may differ significantly from each other.

The difference in the models used in the evaluation also has an effect. The spread of evaluations for ^{240}Pu and ^{242}Pu is shown in review papers [7 and 8] which discuss the SOKRATOR (1975, 1980), ENDF/B-IV, ENDF/B-V (1979), JENDL-I, II (1979) and other evaluations. Evaluations of neutron strength functions cover the range 0.88-1.15 for S_o and 1.22-2.7 for S_1, evaluations of scattering radius R cover the range 8.6-9.2 fm, evaluations of $\overline{D}$ (for ^{242}Pu) cover the range 12.6-16.5. This explains the inadequacy of experimental data on neutron cross-sections for the isotopes under consideration.

Table 2 shows two groups of authoritative evaluations of mean resonance parameters for ^{232}Th, ^{240}Pu and ^{242}Pu documented by the method used to obtain the experimental material analysed and by the quantity of material. These and other evaluations are obtained in order to describe roughly similar experimental information, the examination and analysis of which is beyond the scope of this paper.

From the A-systematics for S_ℓ parameters, we notice that for ^{232}Th the evaluation in Ref. [9] is preferable although the value of R_o is too high. For ^{240}Pu the evaluation in Ref. [11] contains an abnormally low value for R_o and too high a value for S_1. The ENDF/B-V evaluation [12] is more plausible, although it cannot be used in our calculations for ^{242}Pu since the presence of a specially selected "background" in the cross-sections is assumed. At the same time, the evaluation in Ref. [11] is in good agreement with the A-systematics. Thus, in order to calculate the neutron cross-section, we selected the following mean resonance parameters: Pef. [9] for ^{232}Th, [12] for ^{240}Pu and [11] for ^{242}Pu. There are no significant reasons for noticeable departure from the chosen values. We estimate the error in the evaluations adopted to be: $R_o \pm 7\%$, $S_o \pm 10\%$ and the other parameters $\pm 15\%$. This corresponds to an error of 10-15% in the existing experimental data on mean cross-sections.

The <u>results</u> of the authors' calculation for the energy region $E_n \approx$ 1-46.5 keV are given in Table 3, which shows the mean group cross-sections and resonance self-shielding factors, given two dilution cross-sections (σ_o = 0 and σ_o = 100 b) at room temperature. Comparison with other data, for example with the BNAB-78 evaluation [1], has shown that the values for $\langle\sigma_t\rangle$ lie systematically lower than for ^{240}Pu. This is probably due to the low value of R_o in the evaluations of

Ref. [11] on which the BNAB-78 data for ^{240}Pu are based. At the same time, our own mean cross-section data both for ^{240}Pu and ^{242}Pu satisfactorily agree with the ENDF/B-V data (Fig. 1). The authors did not have access to the latest evaluations of group cross-sections for ^{232}Th or the evaluations of group resonance self-shielding cross-section factors for the isotopes studied, apart from the BNAB-78 data [1] for ^{240}Pu. Comparison with the latter (Fig. 2) shows that the effect of resonance self-shielding for ^{240}Pu in Ref. [1] is significantly lower in comparison with the results of the present paper.

Conclusion. Using the latest evaluations of mean resonance parameters for ^{232}Th, ^{240}Pu and ^{242}Pu, group constants are obtained in the region of unresolved resonances (mean cross-sections and resonance self-shielding factors). The results obtained are consistent with the Breit-Wigner formula and the systematics of mean resonance parameters from the optical model. There is lack of experimental data on transmission, which are necessary in order to make a more clearly defined choice of mean resonance parameters and a more accurate definition of resonance self-shielding factors.

REFERENCES

[1] ABAGYAN, L.P., BAZAZYANTS, N.O., NIKOLAEV, M.N., TSIBULYA, A.M., Gruppovye konstanty dlya rascheta reaktorov i zashchity (Group constants for reactor and shielding calculations), Moscow, Ehnergoizdat (1981).

[2] MOLDAUER, B.A., Statistical theory of neutron nuclear reactions. In: Nuclear Theory for Application, Vienna: IAEA, 1980, p.165-186.

[3] IGNATYUK, A.V., LUNEV, V.P., SHORIN, V.S. Raschety sechenij rasseyaniya nejtronov kollektivnymi sostoyaniyami yader metodom svyazannykh kanalov (Calculations of neutron scattering cross-sections for collective nuclear states using the coupled channel method), Voprosy atomnoj nauki i tekhniki, Ser. Yad. Konst. 13 (1974) 59-114.

[4] VAN'KOV, A.A., UKRAINTSEV, V.F., YANEVA, N.B. et al., Analiz ehksperimental'nykh dannykh po propuskaniya nejtronov v oblasti nerazreshennykh rezonansov izotopa ^{239}Pu (Analysis of experimental data on neutron transmission in the region of unresolved resonances for the isotope ^{239}Pu), Soobshchenie P3-83-51 Dubna: OIYaI (1983).

[5] POENITZ, W.P., WHALEN, J.P., SMITH, A.B., Total-Neutron Cross-Sections of Heavy Nuclei, NBS. Spec. Publ. N 594, 1979, p.698-702.

[6] HAOUAT, G., LAGRANGE, Ch., JARY, J. et al., Neutron scattering cross-sections for ^{232}Th, ^{233}U, ^{235}U, ^{239}Pu and ^{242}Pu between 0.6 and 3.4 MeV, Nucl. Sci. and Engng, 1982, v.81, N 4, p.491-511.

[7] WISSHAK, K., KAPPELER, F., Review of the ^{240}Pu and ^{242}Pu Unresolved Resonance Region, INDC (NDS)-129/GJ, Vienna, 1982, p.165-181.

[8] PRONGAEV, V., CULLEN, D.E., Comparison of Strength Functions and Average Level-Spacing for U and Pu Isotopes, INDC (NDS)-129/GJ, Vienna, 1982, p.239-248.

[9] MANTUROV, G.N., LUNEV, V.P., GORBACHEV, L.V., Otsenka nejtronnykh dannykh ^{232}Th v oblasti nerazreshennykh rezonansov (Evaluation of neutron data for ^{232}Th in the region of unresolved resonances), Voprosy atomnoj nauki i tekhniki, Ser. Yad. Knost. I 50 (1983) 50.

[10] VASILIU, G., MATEESCU, S., CHEORGHE, D. et al., Nuclear Data Evaluation for ^{232}Th, INDC (RUM)-10, Vienna, 1980.

[11] ANTSIPOV, G.V., KON'SHIN, V.A., SUKHOVITSKIJ, E.M. et al., Yadernye konstanty dlya izotopov plutoniya (Nuclear constants for plutonium isotopes), Minsk, Nauka i tekhnika (1982).

[12] GARBER, D., Summary Documentation ENDF-201, BNL-17541, 3-ed., UPTION, New York, 1979.

TABLE 1

The results of calculations using the optical model (coupled channel method)

A	R_0, fm*	$S_0 \cdot 10^4$	$S_1 \cdot 10^4$	σ_t, б	σ_{el}, б
232	9,28	I,02	I,7I	I5,8	II,0
238	9,I7	I,00	2,23	I5,7	I0,7
240	9,I3	0,99	2,28	I5,6	I0,7
242	9,I3	0,99	2,62	I5,7	I0,6

* 1 femtometre = 10^{-5} m.

TABLE 2

Evaluations of mean resonance parameters of the three isotopes

Isotope	Reference	R_0, fm	$S_0 \cdot 10^4$	$S_1 \cdot 10^4$	$\overline{D}$, eV	$\overline{\Gamma}_\gamma$, MeV
^{232}Th	/9/	9,65	0,93	I,82	I7,0	20,0
	/I0/	9,72	0,86	I,50	I6,6	20,0
^{240}Pu	/II/	8,58	I,I0	2,80	I3,0	30,7
	/I2/	9,I5	I,04	2,20	I2,7	30,0
^{242}Pu	/II/	9,I4	0,9I	2,50	I4,2	22,2
	/I2/	9,23	0,8I	I,24	I6,5	23,4

TABLE 3

Group constants of three isotopes at dilution cross-sections σ_o = 0 and σ_o = 100 b

Constants	Energy keV				
	I -2,I5	2,I5-4,65	4,65-I0	I0-2I,5	2I,5-46,5
			^{232}Th		
σ_t, б	2I,8	I9,0	I6,8	I5,4	I4,5
σ_c, б	2,03	I,27	0,836	0,56I	0,386
σ_{el}, б	I9,8	I7,8	I6,0	I4,8	I4,2
f_t (0)	0,328	0,42I	0,56I	0,745	0,832
f_t (I00)	0,7I6	0,784	0,886	0,948	0,979
f_c (0)	0,328	0,509	0,702	0,840	0,9I7
f_c (I00)	0,668	0,8I9	0,923	0,970	0,987
f_{el}(0)	0,58I	0,673	0,780	0,872	0,930
f_{el}(I00)	0,773	0,86I	0,933	0,972	0,989
			^{240}Pu		
σ_t, б	22,4	I8,7	I6,5	I4,9	I3,9
σ_c, б	3,05	I,88	I,33	0,980	0,778
σ_{el}, б	I9,0	I6,6	I5,I	I3,8	I3,2
f_t(0)	0,305	0,432	0,560	0,756	0,857
f_t(I00)	0,640	0,772	0,874	0,945	0,976
f_c(0)	0,3I3	0,488	0,693	0,832	0,9I0
f_c(I00)	0,667	0,824	0,924	0,97I	0,987
f_{el}(0)	0,549	0,658	0,759	0,863	0,926
f_{el}(I00)	0,757	0,858	0,926	0,97I	0,988
			^{242}Pu		
σ_t, б	20,7	I7,7	I5,5	I4,5	I3,8
σ_c, б	2,60	I,62	I,I3	0,840	0,638
σ_{el}, б	20,0	I6,0	I4,3	I3,6	I3,2
f_t (0)	0,37I	0,447	0,597	0,703	0,865
f_t (I00)	0,676	0,793	0,899	0,95I	0,978
f_c(0)	0,329	0,527	0,7I2	0,836	0,906
f_c (I00)	0,689	0,84I	0,935	0,973	0,986
f_{el}(0)	0,590	0,680	0,800	0,870	0,929
f_{el}(I00)	0,786	0,869	0,94I	0,973	0,989

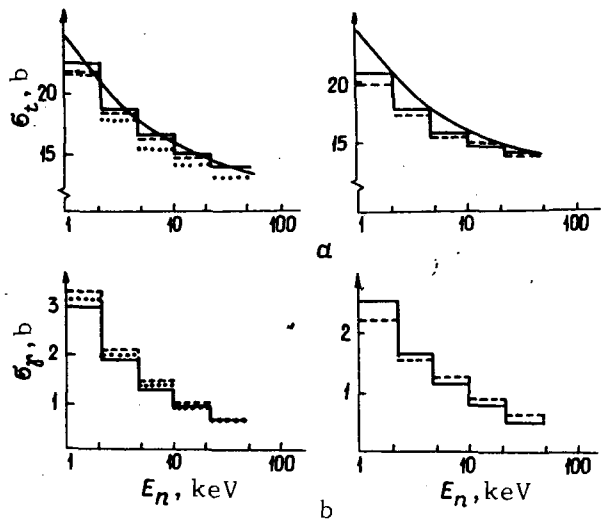

Fig. 1. Group total cross-sections (a) and capture cross-sections (b) of neutrons for nuclei of the isotopes ^{240}Pu (left) and ^{242}Pu (right). Data: ... BNAB-78 [1]; - - - ENDF/B-V [12]; ⌐⌊ calculations by the resonance simulation method (the present paper); ⌊ calculations using the optical model (the present paper).

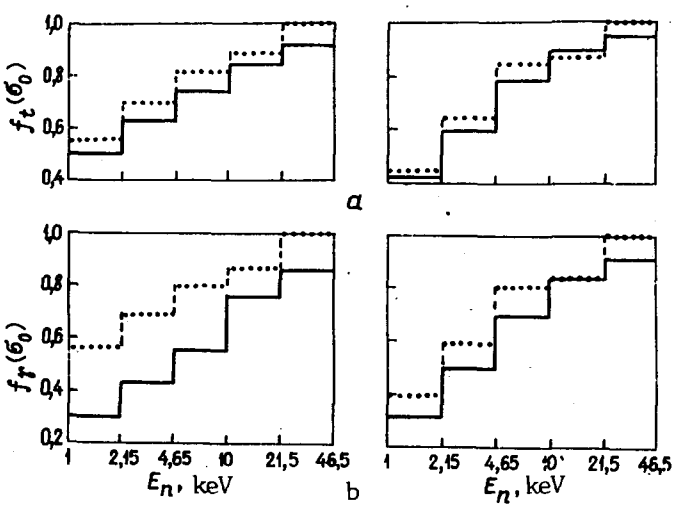

Fig. 2. Resonance self-shielding factors for total cross-section (left) and capture cross-section of ^{249}Pu (right) at 300 K as a function of dilution cross-section σ_0 = 10 (a) and σ_0 = 0 (b). Data: ... BNAB-78 [1]; ⌐⌊ calculations by the resonance simulation method (the present paper).

UDC 539.173.84: 546.791

METROLOGICAL PARAMETERS FOR THE DELAYED NEUTRON METHOD OF ANALYSIS OF GEOLOGICAL STRUCTURES FOR URANIUM

E.G. Vertman

The delayed neutron method has unique metrological parameters for analysis of geological structures with complex matrices (such as rock) [1]. The method is based on recording the delayed neutrons which, in contrast to prompt neutrons accompanying fission of nuclei of heavy elements, have delayed emission. The length of this delay is determined by the half-life of the isotopes, which are called the precursors of the delayed neutrons [2]. Such precursors are fission fragments of the nuclei ^{235}U, ^{238}U and ^{232}Th. The half-lives of the six main groups of isotope-precursors of delayed neutrons range from tenths of a second to a minute.

Delayed neutrons are also emitted by the isotopes $^{9}Li(T_{\frac{1}{2}} = 0.17$ s) and $^{17}N(T_{\frac{1}{2}} = 4.14$ s), but the probability of these isotopes forming when geological structures are irradiated by reactor neutrons is small. From calculations and from Ref. [3] it appears that after a delay of about 20 s after irradiation, the contribution that these isotopes might make to the neutron emission by the sample can be almost completely ignored. In this case, the strength of delayed neutron emission is determined by the uranium and thorium content in the sample studied.

Separate determination of uranium and thorium can be made since ^{238}U and ^{32}Th are fissile when acted on by fast neutrons, whereas ^{235}U is fissile through the action of thermal neutrons. If one takes into account the fact that the natural fractionation of these uranium isotopes is insignificant, and that normally the content of uranium and thorium in rocks is not very different, then by irradiating the same sample first with a neutron flux from the whole reactor spectrum, and then with its epi-cadmium part, one can calculate the uranium and thorium content from the results of these two measurements. By using the experimental reactor channel with the highest ratio of thermal neutron flux to fast neutron flux for purposes of the irradiation, one can measure the uranium content in geological samples during one irradiation. Here both the calculations and the experiment indicate that the thorium contribution may be disregarded.

The method was applied at the IRT-2 research reactor belonging to the Scientific Research Institute for Nuclear Physics at the Tomsk Polytechnical Institute, by using for the purpose the MZN-1 experimental facility; the latter made it possible to evaluate the main possibilities of the method and to analyse more than 30 000 samples for uranium and thorium. The second stage entailed the setting up of an automatic MZN-2U facility at the WWR-K research reactor belonging to the Kazakh Academy of Sciences with an analytical capacity of 45 samples/hour [4].

The simplicity of the analysis operation, measurement operation and calculation of results meant that the whole process could be automated. The basic analysis time scheme is: the sample is irradiated for 60 s, there is 10-20 s delay, then delayed neutrons are recorded for 60 s. When analysing oils and waters the delay is reduced to 10 s, which diminishes the statistical error. The integral delayed neutron count is made by a recording unit with 20 SNM-11 neutron counters and a special 20-channel recording system for excluding instrument error. The result is produced on a digital print-out and calculated by comparing the delayed neutron count from the sample and the standard.

Since there is effective shielding from background neutrons in the physical reactor hall, the facility background is reduced to 30 pulses/min. The maximum sensitivity obtained by the facility is close to the detection level and equal to 5×10^{-7} mass % of uranium with 95% reliability using a 5 g rock sample. The sensitivity of the method can be increased by applying an analysis system in which the sample is unpacked from the capsule containing the sample and measured without it, thereby boosting the recording unit's own background. Another way of improving the sensitivity of the method is to increase the sample mass from 10 to 100 g. However, in this case, the effect of self-shielding must be taken into account.

The content of uranium in crude oils and underground waters without preconcentration by the delayed neutrons method can be determined using high neutron fluxes or by measuring larger samples (up to 1000 g). For oil, the authors used familiar methods of preconcentration by: coking or ashing [5] and production of a solid residue [6]. The main errors inherent in the method lie in the interfering contribution of thorium and in the statistical error. Table 1 shows the dependence of the uranium detection limit on the thorium content in a sample of 10 g, in the case of a recording unit with 20 SNM-1 counters in the MZN-1 facility; given a reactor power of 2.1 MW. For 1 μg of uranium, the integral delayed neutron count is 360 cpm.

The reproducibility of the analysis results using the delayed neutron method is 1-3%, for a uranium content of 10^{-5} is 10%, and less than 10% for a uranium content of 10^{-5}-10^{-6}%. In Ref. [1] the metrological parameters of this method are compared with an extensive range of currently employed methods of analysis. In Table 2 the correlation coefficients are given for the results of the interlaboratory control.

The accuracy of the analytical data using the delayed neutron method is extremely high considering that this method is standardized on the basis of a chemically pure substance (uranyl nitrate) and is a direct method of uranium analysis. This is confirmed by comparison with analysis results of standard rock samples from the USSR and GDR (Table 3).

From what has been stated above, we can conclude that the delayed neutron method of determining the uranium content has high metrological parameters. It enables uranium to be analysed over a wide range of concentrations, which means that the distribution of this element can be studied in the bulk of the varieties of sedimentary, metamorphic and igneous rocks as well as in oils and waters. The significant mass of the sample analysed, together with the high accuracy of the uranium determination method itself, mean that the geothermic aureole may be studied very accurately. The method is a purely instrumental analytical technique, or in other words it is not laborious and therefore involves low costs. It does not require complete pulverization of the sample, crushing to 1-3 mm is sufficient. The method is rapid and can be fully automated.

From the results of uranium content determination in standard rock and ore samples, we can conclude that the "direct" delayed neutron method can be used to analyse standard rock and ore samples over a wide range of uranium concentrations. Comparison of the metrological parameters known at present with the method of determining uranium in geological objects suggests that the delayed neutron method meets the requirements of applied geochemistry much more satisfactorily and opens up for it new prospects.

REFERENCES

[1] VERTMAN, E.G., STOLBOV, Yu.M., MESHCHERYAKOV, R.P., geokhimiya 9 (1979) 1337.

[2] ECHO, M.W., TURK, E.H., PTR-143, Phillips Petroleum, Atom. Energy Division, Idaho Falls, Id., 1957.

[3] AMIEL, S., Anal. Chem., 1962, v. 34, N 13, p. 1683.

[4] VERTMAN, E.G., VAJSHLYA, A.A., SUDYKO, A.F., In "Tezisy Konferentsii" "Molodye uchenye i spesialisty v razvitii proizvoditel'nykh sil Tomskoj oblasti" [In: Conference Proceedings "Young scientists and specialists for the development of production forces in the Tomsk region"], Tomsk, (1980) 187.

[5] ARBUZOV, V.M., IVANTSOV, V.P., KOMOV, V.D., Yaderno-geokhimicheskie metody (Nuclear geochemical methods), Novosibirsk: Izd IGIG SO AN SSSR (1976) 55.

[6] REZNIKOV, A.A., MELIKOVSKAYA, E.P., SOKOLOV, I.Yu., Metody analiza prirodynth vod (Methods for analysis of natural waters), Moscow, Nedra Press, (1970).

[7] SOBORNOV, O.P., Geokhimiya 11 (1977) 1700.

[8] GAVSHIN, V.M., BOBROV, V.A., MALYASOVA, Z.V., Yaderno-geokhimicheskie metody (Nuclear geochemical methods), Novosibirsk, Izd. IGIG SO AN SSSR (1976) 69.

[9] GAVSHIN, V.M., BOBROV, V.A., VERTMAN, E.G., et al. Fizicheskie metody analiza v geokhimii (Physical methods of analysis in geochemistry). Novosibirsk: Izd. IGIG SO AN SSSR (1978) 38.

TABLE 1

Uranium detection limit as a function of thorium content in the sample

Background, cpm	Thorium content, mass %			
	0	10^{-4}	10^{-3}	10^{-2}
For thorium, $N_{\Phi_{th}}$	0	45	450	4500
For analysis				
without capsule (N_{Φ}=26)	$4,3 \cdot 10^{-7}$	$7 \cdot 10^{-7}$	$1,8 \cdot 10^{-6}$	$5,6 \cdot 10^{-6}$
with capsule (N_{Φ_k}=68)	$6,9 \cdot 10^{-7}$	$8,9 \cdot 10^{-7}$	$1,9 \cdot 10^{-6}$	$5,7 \cdot 10^{-6}$

TABLE 2

Comparison of results of rock analysis on uranium, using the delayed neutron method with other methods of analysis

Parameters	Method			
	X-ray fluorescent	Lumi-nescent	Gamma-spectro-metry (with naturally radioactive radium)	Chemical
Correlation coefficient	0,61	0,84	0,72	0,99
Number of analyses	30	30	30	34
Range of uranium content x 10^{-4}%	I-II	I-II	I-II	10^2-10^4

TABLE 3

Uranium content in standard rock samples from the USSR and GDR
$n \cdot 10^{-4}$ mass, %

Standard samples	Manufacturer's data	Delayed neutron method SNIIGG and MS (Tomsk Department)	Gamma-spectrometry method		Instrumental neutron activation analysis IGIG SO AN USSR [9]	Luminescent analysis IGIG SO AN USSR [9]	X-ray fluorescent analysis TsKL MG USSR [9]
			GEOKHI AN USSR [7]	IGIG SO AN USSR [8,9]			
ГІ-С	4,I±0,I	4,6±0,I7	4,6±0,I	-	-	4,05±0,3	-
Г2-С	0,60±0,05	I,05±0,04	0,70±0,05	-	-	0,55±0,07	-
ДІ-С	I,I±0,I	I,3±0,06	I,25±0,05	-	-	0,80±0,07	-
МІ-С	0,I2±0,20	0,27±0,02	-	-	-	0,I2±0,03	-
СТ-ІА	63±4	66,8±0,5	64,9±0,3	77,3±I,3	7I,4±9,7	-	68,I
СТ-ІА	(I)	0,82±0,05	0,80±0,05	0,6±0,05	-	-	I,2
СТД-ІА	(4)	2,4±0,I	2,5±0,I	2,5±0,I	2,2±0,3	-	8,9
СА-І	(I,4÷4,5)	3,I±0,I	3,I±0,I	3,6±0,I	3,I±0,3	-	-
СИ-І	(I,7)	I,5±0,07	I,9±0,I	I,7±0,06	-	-	-
СТ-2	(0,65÷3,0)	0,79±0,05	0,80±0,05	0,6±0,I	0,73±0,I0	-	-
ТВ	3,4±0,6	3,I±0,05	-	3,I±0,2	3,4±0,3	2,70	-
ГМ	6,8±I,5	9,2±0,5	6,6±0,2	8,6±0,3	9,2±0,6	8,45	-
ТS	22	30,5±0,I	-	-	-	-	-
ВМ	(I)	0,85±0,05	0,7±0,I	-	-	-	-
КН	(I)	I,03±0,I	0,8±0,I	-	-	-	-

UDC.539.170.012

NEUTRON SPECTRA FROM THE REACTION (α,xn)

A.V. Balitskij, N.S. Biryukov, B.V. Zhuravlev,
A.P. Rudenko, O.A. Sal'nikov and
V.I. Trukova

This paper is a continuation of the research into energy and angular distributions of neutrons emitted in α-particle induced reactions [1]. Neutron spectra for the (α,xn) reaction were measured for ^{27}Al, ^{53}Cr, ^{56}Fe, ^{58}Ni, ^{60}Ni, ^{62}Ni, ^{90}Zr, ^{91}Zr, ^{94}Zr, ^{113}Cd, ^{115}In, ^{122}Sn, ^{181}Ta nuclei at angles of 30, 60, 90, 120 and 150° with an α-particle energy of 26.8 ± 0.4 MeV. The measurements were made using the time-of-flight method on the cyclotron belonging to the Institute of Physics and Energetics [2]. Metal foils were used as targets. The thickness and isotopic enrichment of the foils is given in Ref. [1]. The average current on the target was 30 nA. The neutrons were recorded with a scintillation detector using a stilbene crystal (diameter 70 mm, thickness 50 mm) and an FEhU-30 photomultiplier with a (n-γ)-discrimination system [3]. The detector efficiency up to 15 MeV was determined by measuring the prompt fission neutron spectra from ^{252}Cf by the time-of-flight method. Above 15 MeV, the efficiency was calculated by the method of direct simulation of the neutron interaction with the scintillator material using the program described in Ref. [4]. The resolution of the spectrometer as determined by the width of the γ-peak at half-height is 1 ns/m for a flight path of 2.5 m.

The characteristic integral spectra and angular distributions of neutrons emitted in the (α,xn) reaction for ^{90}Zr and ^{181}Ta nuclei are given in Figs 1 and 2. The spectra of the asymmetric component of neutron angular distribution is represented by the histogram. Within the limits of measurement error there is agreement between the asymmetrical component spectra and the integral spectra in the high-energy region. This agreement indicates a direct interaction mechanism. Assuming, as in previous publications [1 and 2], that the reaction mechanism represents the sum of the equilibrium and direct components, the neutron emission cross-section may be written as:

$$\sigma(E_n) = A_1 E_n^{5/11} \exp\left[-(12/11)(E_n/T)\right] + A_2 \sqrt{E_n}\, U^{n-1} , \qquad (1)$$

where E_n is the neutron energy; T is the temperature of the nucleus after evaporation of the primary neutron; U is the excitation energy of the nucleus; n is the number of exitons in the residual nucleus; A_1 and A_2 are constants. The first term in Eq. (1), describing the equilibrium decay of the compound system, is the Le Couteur equation [5] derived from the successive particle evaporation model, while the second term is the cross-section for direct interaction obtained from certain assumptions regarding the average matrix element and density states in the residual nucleus [1].

The results of analysing the neutron spectra for the reaction (α,xn) using Eq. (1) are given in Fig. 1 and in the table. The integral spectra and the asymmetrical component and equilibrium emission spectra are in good agreement with the calculations based on Eq. (1) and the parameters given in the table. The best description of the asymmetrical component spectra and corresponding hard part of the neutron spectra is obtained in the majority of cases when n = 3 as well as when E_α = 45 MeV [1]. This corresponds physically to the direct process of stripping during interaction of the α-particles with the nucleus. The divergencies (n = 4 for ^{53}Cr and ^{113}Cd) seem to emphasize the fact that the second term in expression (1) describes only a certain general regularity and does not reflect the individual features of direct interaction. This is also shown by the fairly strong variations in the proportion of cross-sections for non-equilibrium emission at E_α = 45.2 MeV and E_α = 26.8 MeV, coupled with the varied dependence of the average matrix element on the energy of the α-particles.

An important aspect of the analysis is the information it provides on the nuclear level density in the region of high excitation energy obtained from the equilibrium emission spectrum. Having found the temperature of the nucleus T after emission of the primary neutrons using the Le Couteur method [5], we can determine the nuclear level density parameter a:

$$a = \left[(1/T) + (3/2\bar{U})\right]^2 \bar{U} , \qquad (2)$$

where $\bar{U} = E_\alpha - 2T + Q$ is the mean excitation energy of the residual nucleus. The values of the density parameter thus obtained are given in the table. Their generally satisfactory agreement with data of the nuclear level density parameter systematics in Ref. [6] demonstrates the accuracy of the method of dividing the reaction mechanism presented in this paper.

Hence the neutron emission spectra at E_α = 26.8 MeV and at E_α = 45.2 MeV can be interpreted using traditional compound and average direct reaction mechanisms.

Results of analysis of neutron spectra

Nucleus-target	T, MeV	a, MeV^{-1}	n	$\sigma_{\alpha,xn}$, mb	σ_{diz}, mb	$\frac{\sigma_{diz}(45,2)}{\sigma_{diz}(26,8)}$	a $f\sigma$, MeV^{-1}
^{27}Al	2,34±0,03	4,7±0,2	3	776±60	34±3	4,2±0,7	-
^{53}Cr	I,9I±0,02	7,6±0,4	4	2370±I80	I58±20	I,7±0,3	6,5
^{56}Fe	I,86±0,02	6,6±0,3	3	I620±I20	53±6	4,6±0,8	5,8
^{58}Ni	I,86±0,02	5,5±0,3	3	363±30	30±3	5,I±0,9	6,0
^{60}Ni	I,73±0,02	6,7±0,3	3	I270±90	65±6	4,6±0,8	6,6
^{62}Ni	I,76±0,02	7,0±0,4	3	2I80±I60	47±5	7,2±I,3	8,0
^{90}Zr	I,32±0,02	II,5±0,6	3	3I00±230	I3I±I2	2,9±0,5	I0,4
^{91}Zr	I,42±0,02	II,0±0,6	3	3270±240	I0I±I0	4,I±0,7	I0,9
^{94}Zr	I,42±0,02	I0,7±0,5	3	3260±240	I0I±I0	4,4±0,8	I2,0
^{113}Cd	I,3I±0,02	I3,9±0,7	4	2930±220	I07±I2	3,I±0,5	I4,6
^{115}In	I,29±0,02	II,9±0,7	3	2680±200	83±8	4,6±0,8	I4,9
^{122}Sn	I,27±0,0I	I2,6±0,7	3	28I0±2I0	I33±I2	3,7±0,6	I5,3
^{181}Ta	0,94±0,0I	I8,7±I,0	3	2040±I50	66±7	7,5±I,3	I9,8

Note: $\sigma_{d,xn}$ is the total neutron emission of cross-section, σ_{dir} is the cross-section for non-equilibrium emission; a is the nuclear level density parameter in the Fermi-gas model.

REFERENCES

[1] BIRYUKOV, N.S., ZHURAVLEV, B.V., RUDENKO, A.P. et al., Spektry nejtronov iz reaktsij (α,xn). In: Nejtronnaya fizika (Proc. 5th All-Union Conf. on Neut. Phys., Kiev, 15-19 September 1980) Moscow, TsNIIatominform 2 (1980) 30.

[2] BIRYUKOV, N.S., ZHURAVLEV, B.V. et al., Yad. fiz. 31 (1980) 561.

[3] BIRYUKOV, N.S. et al., In: Neutron Induced Reactions (Proc. of the Second Intern. Symp., June 25-29,1979, Smolenice). Bratislava, 1980, p. 435.

[4] CHULKOV, L.V., Preprint No. 2594, Moscow, IAEh (1975).

[5] LE COUTEUR, K.T., LANG, D.W., Nucl. Phys., 1959, v. 13, p. 32.

[6] DILG. W., SCHANTL, W., VONACH, H., Ibid., 1973, v. A217, p. 269.

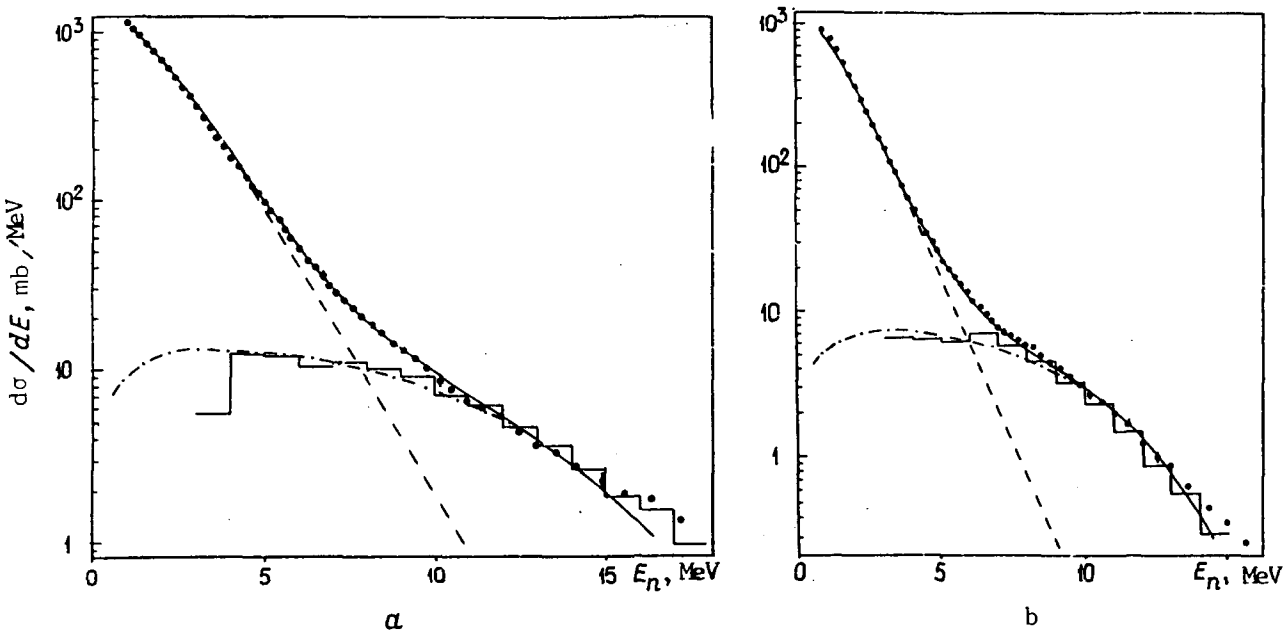

Fig. 1. Neutron spectra for the reaction ^{90}Zr (α,xn) (a) and ^{181}Ta (α,xn) (b). The dots indicate the integral spectrum; the calculated spectra are: - - - equilibrium; -·-· non-equilibrium; —— total; the histogram represents the asymmetrical component spectrum.

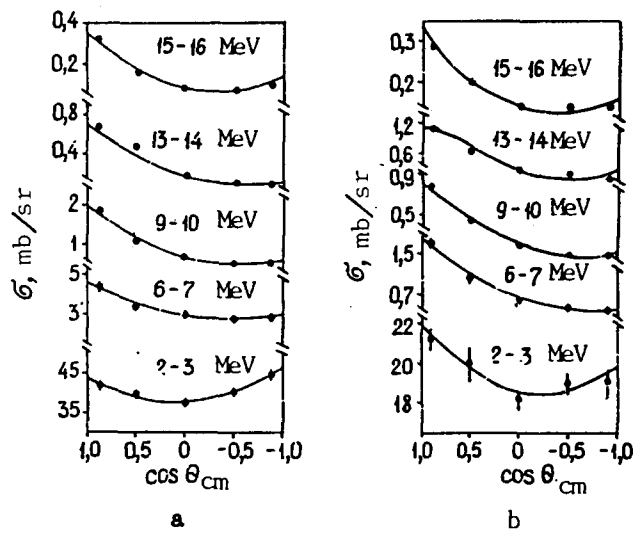

Fig. 2. Angular distributions of neutrons emitted in the reaction (α,xn) for ^{90}Zr (a) and ^{181}Ta (b); the curves indicate approximation by Legendre polynomial expansion.

Bibliographical index of papers in this edition
(International SINDA system)

Element		Quantity	Laboratory	Work-type	Energy (eV)		Page	COMMENTS
S	A				min	max		
LI	006	DEL	FEI	Expt	8.96		I6	Foerch+SIG(NEUT-E),TBL
LI	006	DIN	FEI	Expt	8.96		I6	Foerch+
LI	007	DEL	FEI	Expt	8.96		I6	Foerch+
LI	007	DIN	FEI	Expt	8.96		I6	Foerch+
FE	056	DEL		Expt	1.05	8.05	I9	SARKISØV+ ØPTMØD, GRAPH